INVESTIGATIONS INTO THE ROLES OF PKR-INDUCED ANTIVIRAL STRESS GRANULE AND DHX36 IN RIG-I SIGNALING

Yoo Ji-Seung

Table of Contents

Abstract

Occasionally, living organisms undergo various environmental stresses. Under the stressed conditions, immediate cellular responses are required for maintaining the homeostasis and cell survival.

Virus infection is one kind of cellular stresses that induces a number of cellular responses to counteract this attack. Similar to other types of cellular stresses, viral infection immediately induces cytoplasmic foci, known as stress granule (SG) for protecting from the stresses. Recently, our laboratory found that virus-induced SG plays a critical role in antiviral innate immune responses. We have shown that antiviral proteins such as RIG-I, PKR, OAS1 and RNase L, interact together in the SG. We further showed that type I interferon signaling was inhibited by blocking SG formation, thus we termed this as antiviral SG (avSG).

Although several lines of evidence has been provided for the importance of avSG, the mechanistic relevance to antiviral innate immune response is still unclear. My study is divided into two sections: 1) the significance of virus-induced stress granule in host antiviral responses and 2) the regulatory mechanism of antiviral interferon signaling through antiviral stress granule (avSG). For this purpose, first I examined the relationship between the interferon induction and antiviral stress granule formation. I concluded that antiviral stress granule formation clearly enhances expression of genes encoding IFN and antiviral proteins (Chapter II).

Next, I further studied on the detailed mechanism of avSG-mediated RIG-I signaling. I discovered that DHX36, a putative RNA helicase, interacts with RIG-I and furthermore forms a complex with PKR in virus-infected cells through double-stranded (ds)RNA. In addition, my study elucidated that DHX36 facilitates PKR activation by dsRNA and facilitates avSG formation, finally resulting in augmentation of RIG-I signaling. Antiviral activity of DHX36 was further confirmed using conditional knockout system (Chapter III).

CHAPTER I

INTRODUCTION

1. Thesis overview

The present study described in this thesis aimed to clarify the virus-induced host innate immunity. My study is divided into two sections to examine 1) the significance of virus-induced stress granule on host antiviral responses and 2) the regulatory mechanism of antiviral interferon signaling through antiviral stress granule (avSG). For this purpose, first I examined the relationship between the interferon induction and antiviral stress granule formation and the results are described and discussed in the Chapter II.

Next, I further studied on the detailed mechanism of avSG-mediated RIG-I signaling. I found that DHX36, a putative RNA helicase, interacts with RIG-I and forms a complex with PKR through dsRNA. In addition, my study elucidated that DHX36 facilitates PKR activation and regulates avSG formation, resulting in augmentation of RIG-I signaling. Antiviral activity of DHX36 was further confirmed using conditional knockout system. The details are described and discussed in the Chapter III.

2. Innate immunity and antiviral signaling

Higher vertebrates are capable of inducing memorized immune responses, termed ‘acquired immunity’ (also termed adaptive immunity), by producing specific receptors for non-self molecules, known as antigens. However, this system generally takes almost a week for development of the maximal immunized condition. In contrast, both plant and invertebrates possess distinct immune system and encode a several number of receptors for protecting themselves from foreign pathogenic agents. These receptors recognize conserved molecular patterns associated with microbial pathogens, termed ‘pathogen-associated molecular patterns’ (PAMPs) and are referred to, therefore, as pattern recognition receptors (PRRs). In mammals, similar PRR systems are preserved to respond against pathogen invasion, termed ‘innate immunity’ (Kawai and Akira, 2009) (Kawai and Akira, 2011) (Chen et al., 2009) (Kato et al., 2011). These receptors are germ-line encoded and ubiquitously expressed in most tissues. Since the receptors are expressed in uninfected cells, the innate immune system promptly responds to pathogen infection as a first defense line. When innate immune signaling is triggered, host cells initiate production of a number of inflammatory cytokines and interferon (IFN) to suppress a propagation of pathogens in infected cells and provide an antiviral state for bystander cells, respectively (Ng et al., 2012).

3. RIG-I like receptor

Recent studies have identified several innate immune receptors including retinoic acid-inducible gene I (RIG-I)-like receptors (RLRs), Toll-like receptors (TLRs) and nucleotide-binding oligomerization domain (NOD)-like receptors (NLRs), and clarified their roles in antiviral signaling by sensing viral nucleic acids and proteins leading to induction of cytokines and type I IFNs (Kawai and Akira, 2011). RLRs are putative Asp-Glu-Ala-Asp (DEAD) box containing RNA helicases. RLRs consist of three RNA helicases as a family member that is RIG-I, melanoma differentiation-associated gene 5 (MDA5) and laboratory of genetics and physiology 2 (LGP2), and recent studies elucidated their similar and distinct roles in antiviral responses (Yoneyama et al., 2004) (Yoneyama et al., 2005). Structurally, RLRs consist of three domains: 1) tandem caspase activation and recruitment domain (CARD)-related motif on N-terminus, 2) DExD/H box RNA helicase domain with RNA-dependent ATPase activity on the central region, and 3) C-terminal domain (CTD) that is responsible for recognition of RNA ligands (Fig. 1).

Although all RLRs share the helicase domain and CTD, LGP2 lacks the CARDs that is critical for signal transduction, thus it has been suggested that LGP plays a regulatory role in RLR signaling (Yoneyama et al., 2005) (Satoh et al., 2010).

Similar to other DEAD-box RNA helicases, RLRs contain Walker's ATP-binding motif on the helicase domain and this motif is found to be

essential for function of RLR, suggesting the importance of ATPase/Helicase activity (Yoneyama and Fujita, 2007).

CTD of RLRs is appeared to be involved in recognition of 5'ppp moiety of RNA. Recent studies clarified that CTD contains a positively charged pocket that can accommodate 5'ppp ends of RNA; thus, this property enables RLRs to sense non-self RNAs with 5'ppp (Wang et al., 2010). Because of the structural differences on CTD among the helicases, recognition mechanism of non-self RNA by each helicase differs, resulting in distinct roles in antiviral responses. The exact mechanism of non-self RNA sensing remains to be clarified.

4. RLR signal pathway

In normal condition, RIG-I and MDA5 remain in a 'closed-conformation' representing 'inactive state'. Upon recognition of viral RNAs, RLRs undergo conformational change by ATPase/Helicase activity that results in exposure of CARD domain, representing 'activate state' (Takahasi et al., 2008) (Jiang et al., 2011) (Kowalinski et al., 2011) (Cui et al., 2008). Binding of RLRs to RNA ligands results in the RLR oligomerization for the optimal signaling, thus oligomerization is widely accepted as a hallmark of RLR activation (Peisley et al., 2014). Activated RLRs then transduce the antiviral signaling to downstream signal adapter, interferon promoter stimulator-1 (IPS-1, also termed MAVS, VISA or Cardif) by interaction between RLR and IPS-1 via K63 ubiquitin-mediated CARD-CARD

association (Kawai et al., 2005) (Xu et al., 2005) (Meylan et al., 2005) (Seth et al., 2005) (Sun et al., 2006) (Kumar et al., 2006). Upon interaction, IPS-1 forms a 'prion-like aggregation' on the outer membrane of the certain mitochondria and propagates the antiviral signaling (Hou et al., 2011). It is clarified that mitochondrial dynamics through the mitochondrial 'fusion' and 'fission' is essential for the efficient antiviral signal transduction (Onoguchi et al., 2010).

Aggregation of IPS-1 further recruits multiple ubiquitin ligases, such as TRAFs and TRIMs, and activates several kinase complexes, TBK1/IKKε and IKKα/β/γ to activate transcription factors that initiate induction of antiviral genes (Rajsbaum et al., 2014). Eventually, activation of transcription factors IRF3 and IRF7, as well as NF-kB, leads to the production of type I IFNs and pro-inflammatory cytokines (Kawai and Akira, 2009) (Fig. 2).

Produced IFN-β functions as a messenger of the 'danger sign' from viral invasion. IFN α/β receptors on both IFN-producing and bystander cells received the secreted IFN-β and activate Jak/Stat pathway to induce 'second round' antiviral responses by expressing hundreds of interferon-stimulated genes (ISGs). The antiviral roles of several representative ISGs, such as PKR, OASs and RNase L are well characterized (Ng et al., 2012).

5. RLR agonists

Since viruses utilize distinct and unique strategies in their own life cycles, different types of PAMP RNAs might be generated by different viral infection. Therefore, recognition mechanism of RLRs could be variable by different viral infection. Known RLR-activating molecules are summarized in Table 1.

5-1 RIG-I-activating RNAs

- 5'ppp RNA with secondary structures

  Since 5'ppp moiety is a typical signature of non-self RNA, RNAs containing 5'ppp become an attractive target of antiviral sensors. Indeed, recent studies clarified that RIG-I senses 5'ppp-containing RNAs and induces IFN signaling (Hornung et al., 2006) (Pichlmair et al., 2006). More recently, two groups further elucidated that additional base-paired structures along with 5'ppp is required for RIG-I activation (Schlee et al., 2009) (Schmidt et al., 2009). Since the authors commonly observed that products of in vitro transcription by phage RNA polymerase retained the unexpected 'copy-back' structure; chemically synthesized 5'ppp ssRNA had no effect on the induction of IFN signaling, they concluded that an additional double-stranded region with stem-loop structure is necessary for optimal RIG-I activation. Indeed, several studies confirmed that 5'ppp containing viral genome with secondary structure is truly responsible for triggering antiviral signaling (Rehwinkel et al., 2010) (Fujita, 2009). Furthermore, it was also

reported that defective-interfering (DI) RNA produced by SeV or VSV contains a copy-back structure with 5'ppp and induce RIG-I-mediated IFN signaling (Baum and Garcia-Sastre, 2011) (Panda et al., 2010), suggesting that 5'ppp along with secondary structures is an indispensable characteristic of RIG-I activators.

- Short dsRNA

  Because mammalian cells do not possess a RNA-dependent RNA polymerase, it has been widely accepted that dsRNA is a classical non-self RNA. Indeed, dsRNA, such as poly I:C, is a strong agonist of both RIG-I and MDA5. Unlike IFN signaling by 5'ppp RNA, recognition of dsRNA by RLRs does not require 5'ppp moiety, instead, RNA length is a critical determinant that enables dsRNA to turn on either RIG-I or MDA5 activation (Kato et al., 2008).

  While short dsRNA (< 1 kb) elicits IFN production through RIG-I, long dsRNA (> 7 kb) seems to dominantly activate MDA5-dependent IFN signaling (Kato et al., 2008). These findings were also confirmed by analysis with viral infection. For example, infection with viruses, such as IAV, SeV or VSV that produces undetectable or short dsRNA, activates RIG-I-dependent signaling. In contrast, long dsRNA-producing virus, such as EMCV, induces IFN signaling through MDA5. Intriguingly, Reovirus that possesses different-sized segmented dsRNA in the

viral particle is recognized by both RIG-I and MDA5, confirming the length-dependent recognition of dsRNA by RLRs.

- Sequence-specific RNA sensing by RIG-I

  In addition to non-self biochemical property of PAMP RNAs, RNA sequence is also one of important signature of RIG-I agonist. Recently, Saito et al. observed that HCV genome possesses U/UC-rich RNA in its 3' UTR and they further found that RNA containing 5'ppp along with U/UC-rich sequence is a potent RIG-I activator (Saito et al., 2008). In addition, Davis et al. also discovered that AU-rich sequence in IAV 3'UTR is recognized by RIG-I (Davis et al., 2012). However, unlike HCV U/UC-rich RNA, 5'ppp is dispensable for recognition of IAV-derived AU-rich RNA by RIG-I, suggesting the involvement of distinct mechanism for sequence-specific RNA sensing.

  Sensing of AU-rich RNA by RIG-I is also important for recognition of cytoplasmic dsDNA. Recent studies suggested that AT-rich dsDNA triggers IFN signaling through the RIG-I pathway (Ablasser et al., 2009) (Chiu et al., 2009). It was demonstrated that dsDNA containing AT-rich, but not GC- or IC-rich, became a template for RNA polymerase III that produces 5'ppp-containing AU-rich RNA. Since these RNA transcripts are perfectly complementary to each other, 5'ppp-containing AU-rich dsRNA

might be generated by self-annealing and trigger RIG-I-dependent IFN signaling.

- Products of RNase L

  It is reported that host ribonuclease augments RLR signaling. In 2007, Malathi et al discovered that small RNAs produced by cleavage of both host and viral RNA by RNase L can potentiate interferon signaling by RLRs (Malathi et al., 2007). Upon viral infection, RNase L is activated by 2', 5'-linked oligoadenylate, which is generated by activated OAS1, and cleaves all RNAs including host and viral RNAs in the cells. Cleaved products are 5'-hydroxyl (5'-OH) and 3'-monophosphoryl (3'-P) group containing small RNAs (< 200 nt) and become a ligand of both RIG-I and MDA5. Since IFN signaling is abolished by removal of 3'-monophosphate of cleaved RNA, RLRs may also recognize 3'-p moiety of certain RNAs. Additionally, the authors further suggested the requirement of a higher order structure for sensing of those 3'-p RNAs by RLR (Malathi et al., 2010).

5-2 MDA5-activating RNAs

- Long dsRNA

  Although little is known for MDA5-activating RNA ligands, recent studies suggested several known characteristic of MDA5 agonists. It is found that MDA5 mainly recognizes positive single-

stranded RNA viruses, such as picornaviridae, caliciviridae, togaviridae and flaviviridae family member as well as dsRNA virus such as reoviridae member. Notably, these viruses commonly produce or possess ‘long dsRNA’ during their life cycles, thus it is widely accepted that MDA5 senses long dsRNA. Indeed, Feng et al also proved that MDA5 senses neither genomic RNA nor viral mRNA, but recognizes the replication intermediates produced during minus-strand genome synthesis (Feng et al., 2012), further supporting the notion that long dsRNA is a critical feature of the MDA5 agonist.

- RNA web

  In addition to length dependency, RNA structure is also significant feature of the MDA5 ligand. Recently, it is suggested that activation of MDA5 requires a ‘high-order’ RNA structure (Pichlmair et al., 2009). Surprisingly, purely long dsRNA (> 10 kb) generated by EMCV or VV does not activate IFN signaling even though MDA5 interacts with it. However, both ss- and dsRNA containing huge RNA, termed ‘high molecular weight (HMW)’, induces robust innate immune responses. Since the authors confirmed that RNA sequence is not involved in this regulation, they concluded that MDA5 activation requires a ‘RNA web’ rather than just ‘simply long’ dsRNA.

- Cleaved viral mRNA

  Recent study also suggested that MDA5 is capable of sensing PIV5 mRNA (Luthra et al., 2011). The authors showed that PIV5 mRNA coding L protein is cleaved by RNase L and becomes a potent ligand of MDA5. In this regulation, MDA5 seems to recognize specific sequence of PIV5 mRNA because only certain region of viral mRNA activates MDA5.

6. PKR, a protein kinase with multiple functions

   Along with RLRs, PKR is a representative cytosolic foreign RNA sensor playing a pivotal role in regulating innate immune responses (Balachandran and Barber, 2007) (Gilfoy and Mason, 2007) (McAllister et al., 2010) (Pindel and Sadler, 2011) (Schulz et al., 2010) (Sen et al., 2011). PKR consists of two domains: N-terminus dsRNA binding domain and C-terminus domain with kinase activity. Like RLRs, PKR specifically recognizes non-self RNAs such as dsRNA or 5'ppp containing secondary-structured RNA (Schlee et al., 2009) (Nallagatla et al., 2007). Upon non-self RNA recognition, PKR dimerizes and autophosphorylates, resulting in active state of PKR.

   PKR plays a number of cellular responses by various stimulations. For example, PKR exerts its anti-cancer activity by direct interaction with tumor repressor, p53 (Cuddihy et al., 1999). Moreover, PKR is involved in activation of MAP kinase signaling (Goh et al., 2000). Furthermore, recent study suggested that PKR plays a critical role in

inflammasome activation induced by various environmental stresses (Lu et al., 2012). The best-studied PKR function is related to its antiviral activity. It is well known that PKR inhibits virus replication by limiting the protein synthesis in virus-infected cells. Since PKR is a one of four eIF2α kinases, dsRNA-induced PKR activation rapidly phosphorylates eIF2α, leading to inhibition of both host and viral protein translation, resulting in antiviral responses. Moreover, PKR also contributes to antiviral responses by activating NF-κB signaling through destabilizing IKK complex that allows NF-κB translocation to the nucleus (Garcia et al., 2006). More recently, Schulz et al suggested that PKR regulates IFN signaling by regulating the integrity of IFN mRNA (Schulz et al., 2010). However, although accumulating evidence has suggested that PKR has an important role in antiviral host defense, the exact mechanisms underlying the regulation of innate immunity remain to be elucidated.

7. Stress granule and antiviral stress granule

   Eukaryotic cells exhibit temporal and dynamic aggregates in the cytoplasm under various environmental stresses such as UV, heat shock, starvation, chemicals, ER- and oxidative stresses, and virus infection, etc, thus termed stress granules (SG). The best characterized model for SG formation involves phosphorylation of the translation initiation factor eIF2α by protein kinase PKR, PERK, GCN2 and HRI (Anderson and Kedersha, 2002). Because SG contains 48S

translation pre-initiation complexes together with number of RNA binding proteins, it has been suggested that SG is a place where translation is arrested under stress conditions (Anderson and Kedersha, 2008). However, since hundreds of molecules are involved in SG assembly, the biological function and molecular mechanism are poorly understood.

Recently, increasing number of studies has suggested the significance of SG for antiviral responses. We as well as others have shown that PKR plays essential role for the virus infection-induced SG formation. We further clarified that SGs provide a critical platform for interactions between antiviral proteins and non-self RNA ligands thus termed antiviral SG (avSG) (Ng et al., 2013) (Okonski and Samuel, 2013) (Onomoto et al., 2012) (Simpson-Holley et al., 2011) (Fung et al., 2013). Consistent with our observation, recent study also proved that PAMP RNA is localized in SG and IFN induction was dependent on PKR under this condition (Witteveldt et al., 2014).

A tight link between SGs and antiviral innate immunity has been suggested by multiple studies. Indeed, it is shown that most viruses appear to inhibit SG formation through multiple strategies for the evasion of host antiviral responses (Valiente-Echeverria et al., 2012) (White and Lloyd, 2012) although several viruses conversely utilize it during their viral life cycles (Ariumi et al., 2011) (Carroll et al., 2014).

8. DHX36, a putative RNA helicase

DExD/H-box helicase 36 (DHX36), also termed RNA helicase associated with AU-rich RNA element (ARE) (RHAU) was originally identified as a factor involved in ARE-mediated mRNA decay with exosome components by screening analysis with AU-rich RNA as a bait (Tran et al., 2004).

DHX36 consists of three domains that: 1) RNA binding domain on its N-terminus, 2) central helicase domain with ATPase/Helicase activity, and 3) C-terminal domain with unknown function. Through N-terminal RNA binding domain with helicase activity, DHX36 can directly interact with and unwind the specific structure of guanine-tetramolecular quadruplex-DNA or -RNA (G4-DNA or G4-RNA) and this G4-resolvase activity regulates the transcription of gene containing G4 structures (Creacy et al., 2008) (Lattmann et al., 2010). It is also reported that DHX36 associates with SG in response to various cellular stresses and RNA binding affinity by N-terminal domain is required for the recruitment of DHX36 to SG (Chalupnikova et al., 2008).

Recently, DHX36 has also been suggested as a critical regulator of antiviral host immune responses. For example, it is reported that DHX36 functions as a foreign DNA sensor in plasmacytoid dendritic cells (pDC) (Kim et al., 2010). Moreover, it has been also suggested that DHX36 play a pivotal role in dsRNA-induced IFN signaling by forming a complex together with other RNA helicases and TRIF, a signal adapter, indicating the multiple roles of DHX36 in biological responses (Zhang et al., 2011).

CHAPTER II

ANTIVIRAL STRESS GRANULE ENHANCES INNATE IMMUNE SIGNALING

1. Chapter introduction

Cellular responses to environmental stresses are critical for maintaining homeostasis in living organisms. Eukaryotic cells promote rapid formation of cytoplasmic aggregates with RNA and multiple RNA-binding proteins termed stress granules (SGs). Over the past decade, SGs have been suggested to be critical compartments and play essential roles in cellular responses against various environmental stresses.

We have previously reported that virus infection induced SG-like aggregates and are crucial for antiviral response, therefore termed them as antiviral (av) SGs. However, exact mechanism and functional relevance on innate immune responses are still required to be clarified. In this chapter, I tried to elucidate the functional significance of avSG-mediated IFN signaling through the biochemical and molecular biological assays for better understanding of our innate immune system induced by virus infection. The data in this chapter describe the significant role of PKR-mediated avSG formation in maximal antiviral responses.

2. Results

2-1 PKR regulates avSG formation and IFN signaling

Recently our group reported that viral infection-induced SG is formed in a PKR activation-dependent manner and is a critical place for PAMP recognition and antiviral signal transduction, thus termed avSG. To further elucidate the significance of avSG, first, I re-confirmed the function of PKR on avSG-mediated IFN signaling by transfection of poly I:C to SG reporter HeLa cell that stably expressing GFP-tagged G3BP1 (GFP-G3BP HeLa, ref), a typical marker of SG. Transfection of poly I:C strongly induced the phosphorylation of PKR (Fig. 3A). Consistent with our previous data, poly I:C-transfected cells induced robust avSG formation and expression of IFN-β mRNA in a PKR-dependent manner (Fig. 3B and 3C), confirming the significant role of PKR in avSG-mediated IFN signaling.

2-2 RNA length-dependent induction of the expression of antiviral proteins

To further study on the mechanistic relevance between avSG and host innate immune responses, I utilized three types of RNAs in different lengths (27-, 86- and 136-nt) produced by in vitro transcription (Fig. 4A). Transfection of ivt-RNA induced expression of antiviral proteins such as RIG-I, MDA5 and PKR (Fig. 4B). While PKR level was comparable among RNA-

transfected samples, expression of RIG-I and MDA5 was increased in a RNA length-dependent manner. Moreover, level of phosphorylated PKR was much higher in the cells transfected with longer ivt-RNA, 5'ppp 136, suggesting that RNA length is an important determinant for the expression and activation of antiviral proteins.

2-3 avSG enhances antiviral signaling

Because level of PKR phosphorylation was elevated in a RNA length-dependent manner, next I monitored the formation of avSG by those RNAs using GFP-G3BP1 Hela cells. Consistent with PKR phosphorylation, transfection of 5'ppp 136 strongly induced avSG formation. However, 5'ppp 27 or 86-transfected cells did not exhibit the avSG formation (Fig. 5A) even though phosphorylation of PKR was detected (Fig. 4B), suggesting that a certain level of phosphorylated PKR is required for triggering of avSG formation. Expression of IFN-β and IL-8 mRNA was also affected by length of RNA ligands. Notably, level of IFN-β and IL-8 mRNA was much higher in 5'ppp 136-transfected cells compare to that induced by 5'ppp 27- or 86 (Fig. 5B). Consistently, higher level of IRF3 dimer was detected by stimulation with avSG-inducing RNA such as poly I:C (Fig. 3B) or 5'ppp 136 compare to that with 5'ppp 27 (Fig. 5A), indicating the significant role of avSG in enhancement of antiviral signaling (Fig. 5C). It is reported that oligomerization of

RIG-I is critical for optimal induction of IFN signaling (Peisley et al., 2014). To check if formation of avSG is related to RIG-I oligomerization, Native-PAGE was performed with RNA-transfected HeLa stably expressing FLAG-RIG-I. Interestingly, while transfection of avSG-inducing RNA ligands, poly I:C and 5'ppp 136, clearly induced the oligomerized RIG-I, RIG-I remained as monomer by 5'ppp 27, suggesting that formation of avSG facilitates RIG-I oligomerization (Fig 5D). Altogether, these results demonstrate that although avSG is not absolutely required for triggering of antiviral responses, RIG-I activation and subsequent antiviral signaling was enhanced by avSG.

2-4 PKR regulates IFN signaling in a ligand-dependent manner

Because PKR regulates IFN signaling through induction of avSG, next I asked if PKR is also involved in IFN signaling induced under non-avSG condition. To address this, the level of IRF3 dimerization was examined using control or PKR knockdown HeLa cells by transfection of 5'ppp RNAs or poly I:C. Poly I:C- and 5'ppp 136-induced IRF3 dimer was significantly reduced by PKR depletion (Fig. 6A and 6B). In contrast, the level of IRF3 dimerization by 5'ppp 27 was not affected by deletion of PKR, confirming the avSG-mediated IFN signaling by PKR.

2-5 5'ppp moiety is not required for avSG-mediated antiviral signaling

Because ivt-RNA contains triphosphophate group on its 5' end (Schlee et al., 2009) (Schmidt et al., 2009); PKR can also recognize 5'ppp containing stem-loop structured RNA (Nallagatla et al., 2007), next I asked if 5'ppp is required for avSG-mediated immune responses. To answer this, formation of avSG was monitored by transfection of normal or phosphatase-treated 5'ppp RNAs in GFP-G3BP1 HeLa cells. As shown in Fig. 7A, 5'ppp 136, but not 5'ppp 27, induced avSG. Interestingly, phosphatase treated-5'ppp 136 is still capable of inducing cytoplasmic foci, indicating that 5'ppp is dispensable for the formation of avSG (Fig. 7A). Next, level of IFN-β and IL-8 mRNA was evaluated. 5'ppp 27-induced IFN-β mRNA level was dramatically decreased by dephosphorylation. However, expression of IFN-β mRNA by 5'ppp 136 was modestly affected by phosphatase treatment (Fig. 7B, IFN-beta). Interestingly, while 5'ppp 27 barely induced the expression of IL-8 mRNA, robust induction of IL-8 mRNA was observed in 136-nt RNAs (5'ppp 136 and 5'ppp 136-CIAP) regardless of 5'ppp moiety (Fig. 5B and Fig. 7B, IL-8), suggesting the involvement of distinct mechanisms in triggering of different cytokine production through the avSG-dependent or -independent pathway. Collectively, these data demonstrate that 5'ppp is not essentially required for the avSG-mediated innate immune responses.

3. Discussion

We have been suggesting that virus-induced SG is a crucial for antiviral sensors to recognize PAMP RNA and transduce the antiviral signaling (Onomoto et al., 2012) (Ng et al., 2013) (Fung et al., 2013). We found that antiviral proteins including RLRs, PKR, OAS, and RNase L were co-localized with conventional SG markers and interacted with viral RNA. Moreover, we clarified that virus-induced SG formation is absolutely dependent on activation of PKR and deletion of PKR completely inhibited virus- or dsRNA-induced SG resulting in failure of antiviral signaling, thus we termed this virus-induced SG as an antiviral SG. However, since numerous proteins are interacting within the SG; yet no distinct signatures between 'conventional' and 'antiviral' SG have been defined, more work is required to completely understand the precise molecular mechanisms of avSG-mediated innate immunity.

In the current study, I examined the significant role of avSG in the host innate immune responses. Since it is reported that length and 5'ppp moiety with secondary is a critical signature of PKR ligands, I utilized several RNA ligands in different lengths produced by in vitro transcription with or without phosphatase treatment to further analyze PKR:avSG-dependent regulation.

My study revealed that RNA length is a critical signature for regulation of innate immunity. Western blot analysis showed the distinct expression pattern of several antiviral proteins by different RNA

ligands. For example, the expression level of RIG-I and MDA5 was elevated in a RNA-length dependent manner. However, the expression of PKR was not affected by RNA length. In contrast, level of PKR phosphorylation was dramatically increased upon stimulated by longer RNA (Fig. 4).

Next, I also proved that RNA length is important for inducing avSG formation and antiviral signaling. Among three RNAs tested, only longer RNA (5'ppp 136) had a potential to induce formation of avSG (Fig 5A). Furthermore, induction of IFN-β and IL-8 mRNA (Fig. 5B) as well as IRF3 dimerization (Fig. 5C) was dramatically increased by longer RNA compare to other two shorter RNAs, suggesting the important role of avSG in enhancing the antiviral signaling.

Recently, Patel et al suggested that oligomerization of RIG-I occurs through its ATPase activity and is required for optimal RIG activation (Patel et al., 2013). Moreover, Jiang et al. also reported that ubiquitin-induced RLR oligomerization is critical for downstream signal transduction (Jiang et al., 2011) (Jiang et al., 2012). In agreement with previous findings, my data confirmed the RIG-I oligomerization by RNA transfection. Interestingly, oligomerization of RIG-I was only detected by avSG-inducing RNA ligands (Fig. 5D). Based on this data, it is tempting to speculate that avSG may serve a place for interaction between antiviral proteins and signaling molecules that is involved in RLR oligomerization such as E3 ubiquitin ligases, and facilitates efficient RIG-I oligomerization for maximal IFN signaling (see

hypothetical model in Fig. 8). For this model, it would be more convincing if TRIM25, an E3 ubiquitin ligase and a known RIG-I activator (Gack et al., 2007), co-localizes with RIG-I in avSG.

Finally, I provided significant evidence that distinct RNA sensing mechanism(s) is involved in antiviral signaling using 5'ppp- or dephosphorylated-RNA. It is well known that ivt-RNA contains 5'ppp moiety with copy-back structure and triggers RIG-I-dependent IFN signaling (Schlee et al., 2009) (Schmidt et al., 2009). Consistent with previous observation, my data confirmed that removal of 5'ppp from short RNA failed to activate antiviral signaling (Fig. 7B, 5'ppp 27 and 5'ppp 27-CIAP). Interestingly, only modest reduction of IFN-β mRNA level was detected by phosphatase-treated 5'ppp 136 compare to normal 5'ppp 136 (Fig. 7B, 5'ppp 136 and 5'ppp 136-CIAP). Notably, removal of 5'ppp did not affect induction of IL-8 mRNA. Moreover, the formation of avSG was still similarly induced by phosphatase-treated 5'ppp 136 compare to that stimulated by normal 5'ppp 136 (Fig. 7A, 5'ppp 136 and 5'ppp 136-CIAP), suggesting that avSG-mediated antiviral signaling does not require 5'ppp moiety. In fact, it has been suggested that 5'ppp is not essential for IFN induction by dsRNA (Kato et al., 2011). Indeed, poly I:C does not possess 5'ppp. This notion is consistent with our previous finding that RIG-I undergoes a different type of conformational change when bound to poly I:C in comparison to 5'-ppp RNA (Takahasi et al., 2008).

Altogether, my data here suggest that the mechanism of RIG-I activation by at least two types of RNA ligands might be fundamentally different and that is possibly through avSG-dependent and -independent regulation.

CHAPTER III

DHX36 REGULATES RIG-I SIGNALING BY FACILITATING PKR-MEDIATED ANTIVIRAL STRESS GRANULE FORMATION

1. Chapter introduction

In the previous chapter, I described the importance of avSG for the host innate immune responses by RIG-I. In this chapter, I further demonstrate that another DExD/H-box RNA helicase DHX36 is a key molecule for RIG-I signaling by regulating PKR activation. I found that DHX36 directly interacts with RIG-I and forms an antiviral complex with PKR in a dsRNA-dependent manner. By forming this complex, DHX36 facilitates dsRNA binding and phosphorylation of PKR through its ATPase/helicase activity. Using DHX36 KO-inducible MEF cells, I also found that DHX36 deficient cells showed defect in IFN production and higher susceptibility in RNA virus infection, indicating the physiological importance of this complex in host defense.

In this chapter, I will describe about the novel function of DHX36 on the regulation of PKR-dependent avSG formation that facilitates RIG-I-mediated antiviral signaling.

2. Results

2-1 DHX36 KO-inducible system in MEF

Because knockout of DHX36 gene caused a fatal mortality in mouse, tamoxifen-induced conditional DHX36 KO system was established (Lai et al., 2012). To examine the function of DHX36 in the RIG-I-mediated IFN signaling, I adopted the conditional DHX36 KO MEF system for further study. First, the efficiency of tamoxifen-induced deletion of the *dhx36* gene was evaluated (Fig. 9). After 72 h treatment of tamoxifen, level of DHX36 became undetectable, thus this condition was chosen for inducing the DHX36 KO.

2-2 DHX36 regulates IFN signaling in a stimulus-dependent manner

Next, the involvement of *dhx36* KO in IFN-ß gene activation was evaluated. Protein level of IFN-ß induced by infection with influenza A virus (IAV) ΔNS1, Newcastle disease virus (NDV) or by transfection of poly rI: poly rC (pIC) was significantly decreased in the DHX36 KO MEF (Fig. 10A-C). In contrast, 5'ppp 27-induced IFN signaling was not affected by deletion of DHX36 (Fig. 10D). Consistent results were obtained by qPCR analysis by checking the IFN-ß mRNA level (Fig. 11A-D), suggesting that DHX36 plays a significant role in RIG-I-mediated antiviral signaling in a stimulus-dependent manner.

2-3 DHX36 regulates IFN signaling through IRF3 activation

Recently, it is reported that DHX36 is required for dimerization of IRF3 by dsDNA or dsRNA stimulations in dendritic cells (Kim et al., 2010) (Zhang et al., 2011). Thus, next I checked whether DHX36 also regulates IRF3 dimerization for the optimal antiviral signaling in MEF. While knockout of DHX36 profoundly diminished the dimer form of IRF3 by NDV infection, comparable level of IRF3 dimerization was detected by 5'ppp 27 stimulation, confirming the stimulus-dependent involvement of DHX36 in antiviral signaling (Fig. 12A). In NDV-infected HEK293T cells, knockdown of DHX36 significantly decreased active IRF3 dimers (Fig. 12B). Since NDV replication was comparable up to 12 hr (Fig. 12C and Fig 11B) by the presence or absence of DHX36, the data suggest the involvement of DHX36 in antiviral signaling through activation of IRF3.

2-4 DHX36 co-localizes with antiviral proteins in avSG

Recently, it is reported that DHX36 localizes in SGs induced by various stresses (Chalupnikova et al., 2008). To check if DHX36 also localizes in virus infection-induced SG, immunostaining analysis is performed with IAVΔNS1-infected HeLa cells. As we reported (Onomoto et al., 2012), I confirmed that infection of HeLa cells with IAVΔNS1 induced foci of SG marker T-cell intracellular antigen-1-related protein (TIAR) and these granules also co-

localized with RIG-I and IAV nucleocapsid protein (NP) (Fig. 13A). Co-localization of the proteins was also quantified and presented with a bar graph in Fig. 13A. In normal condition, DHX36 is diffusely distributed in both the nucleus and cytoplasm. However, IAV∆NS1 infection induced its re-localization to speckles, which co-localized with RIG-I and TIAR (Fig. 13B). Quantification data showed that co-localization of DHX36/TIAR and DHX36/RIG-I was highly inducible and was observed in the majority of speckles (~90 %, bar graph in Fig. 13B). Since PKR is a key molecule for induction of avSG (Fig. 3, ref), I also monitored co-localization of PKR with RIG-I in avSGs induced by infection with IAV∆NS1 (Fig. 13C). Collectively, these results confirmed that DHX36, RIG-I, PKR and TIAR localizes in avSGs by virus infection.

2-5 DHX36 interacts with antiviral proteins

Because my data showed that DHX36 co-localized with RIG-I and PKR, I examined their physical interaction by co-immunoprecipitation (IP). HEK293T cells were transfected with expression vector for full-length RIG-I or RIG-I∆CTD, which lacks the C-terminal domain (CTD). After mock or IAV∆NS1 infection for 12 h, physical interaction was examined by co-IP. DHX36 interacted with RIG-I through the C-terminal domain of RIG-I regardless of virus infection (Fig. 14A). In contrast, interaction between PKR and RIG-I was dependent on virus infection. In

addition, RIG-I CTD was partly responsible for this interaction. Notably, since no DHX36 association was detected by co-IP with RIG-IΔCTD, it is likely that DHX36 may facilitate the interaction between RIG-I and PKR. To further confirm that interaction between DHX36 and RIG-I does not require the viral infection in MEF, co-IP was performed using FLAG-RIG-I stably expressing *rig-i* null MEF. Consistently, the interaction between DHX36 and RIG-I was occurred without any stimulation, confirming their constitutive interaction (Fig. 14B).

2-6 DHX36 interacts with RIG-I through its helicase domain

It is reported that DHX36 consists of three domains: N-terminus RNA binding domain, helicase domain, and C-terminus domain with unknown function (Chalupnikova et al., 2008). Since DHX36 directly interacts with RIG-I CTD, next I asked which domain of DHX36 is responsible for this interaction. To answer this, co-IP analysis was performed using GFP-tagged WT or deletion mutants of DHX36 together with FLAG-tagged RIG-I. Consistent with my previous data (Fig. 14), WT DHX36 interacted with RIG-I (Fig. 15). Co-IP analysis further revealed that neither N-terminus nor C-terminus, but helicase domain was responsible for the interaction with RIG-I (Fig. 15).

2-7 DHX36 binds to dsRNA and forms a complex with antiviral proteins

Because DHX36 co-localizes with antiviral proteins in avSG upon viral infection, next I asked if DHX36 forms an antiviral complex through the RNA ligands. To address this question, I performed poly I:C pull-down analysis using an extract from uninfected cells (Fig. 16A). The result clearly showed that DHX36 has binding affinity to dsRNA in addition to AU-rich RNA, as reported previously (Tran et al., 2004). RIG-I and PKR also bound to the dsRNA and presumably forms a RNP complex. However, TIAR, a SG component and a known RNA binding protein, did not show binding affinity to the dsRNA, suggesting that interaction among DHX36, RIG-I and PKR in avSGs is dsRNA specific. Purified recombinant DHX36 exhibited clear binding with pIC (Fig. 16B), demonstrating the direct interaction between DHX36 and dsRNA. Altogether, these data strongly suggest that DHX36 forms a complex with antiviral proteins through dsRNA.

2-8 DHX36 recognizes IAV RNA

To further examine whether DHX36 recognizes viral RNA, I performed RNP-IP analysis using anti-DHX36 monoclonal antibody to pull down endogenous DHX36-RNA complex. Efficiency of RNP pull down was confirmed by Western blot analysis and direct interaction between DHX36 and RIG-I was

confirmed again (Fig. 17A). Then, total RNA was isolated from RNP complex and utilized for real-time qPCR to evaluate interaction between DHX36 and IAV viral RNAs. qPCR analysis revealed that DHX36 associates with viral RNAs (Fig. 17B). Among the viral RNAs examined, IAV segment 8 was the strongest ligand of DHX36 (Fig. 17C). Next, localization of IAV RNA was monitored using IAVΔNS1-infected HeLa cells by confocal microscopy. Because IAV produces viral RNAs containing partial double-stranded panhandle-structure (Fujita, 2009), propidium iodide (PI), which specifically binds to both dsDNA and dsRNA, was utilized for staining of the cytoplasmic dsRNA. IAVΔNS1 infected cells exhibited the cytoplasmic granules stained by PI and these foci were co-localized with RIG-I and DHX36 (Fig. 18). Collectively, these results suggest that DHX36 and RIG-I directly recognizes viral RNAs in the avSG.

2-9 Localization of TRIM25 to avSG

To further prove the functional relevance of avSG to host antiviral responses, I monitored the localization of TRIM25, which is widely accepted marker of RIG-I activation (Gack et al., 2007) using virus-infected or poly I:C-transfected HeLa cells. TRIM25 is normally distributed diffusely in the cytoplasm. Intriguingly, virus-infected or pIC-transfected cells exhibited translocation of TRIM25 to avSG together with DHX36 and G3BP1 (Fig. 19A). To confirm

that avSG is distinct from conventional SG, we induced oxidative stress in the cells by treatment of arsenite that strongly induces SG. Arsenite-treated cells showed a robust formation of SG, however TRIM25 was not localized in SG induced under this condition (Fig. 19B), which did not induce IFN signaling (Fig. 19C). Thus, these data strongly suggest that interaction between TRIM25 and antiviral proteins in the avSG is critical for the efficient antiviral signaling.

2-10 DHX36 mediates avSG formation

To explore the underlying mechanism of DHX36 requirement in IFN signaling, formation of avSG was monitored using control or DHX36-depleted HeLa cells by viral infection. Interestingly, IAVΔNS1-induced avSGs was inhibited by DHX36 depletion. Furthermore, reduction of nuclear translocation of IRF3 was also detected (Fig. 20A) in a DHX36-knockdown cells. Consistently, NDV-induced avSG was also markedly diminished by DHX36 knockdown (Fig. 20B). Since DHX36 deletion did not affect viral RNA production up to 12 h (Fig. 12C), these data demonstrate that DHX36 plays a significant role in the regulation of IFN signaling by mediating avSGs formation.

2-11 DHX36 affects interaction between RIG-I and SG component

We previously reported that RIG-I associates with G3BP1 in an IAVΔNS1 infected cells (Onomoto et al., 2012). Thus, I examined the association of RIG-I and G3BP1 in NDV-infected GFP-G3BP1 HeLa cells by co-IP analysis. Interestingly, interaction between RIG-I and G3BP1 was significantly attenuated by DHX36 knockdown (Fig. 21). Moreover, aggregation of G3BP1 was also inhibited by depletion of DHX36 (Fig. 21, see endogenous G3BP). Since efficiency of co-IP was comparable in both control and DHX36-depleted samples (Fig. 21, see GFP), these data indicate that DHX36 mediates the association of RIG-I with SG component.

2-12 DHX36 is required for optimal activation of PKR

It has been suggested that different stresses activate one of the four distinct eIF2α kinases, such as PERK, HRI, GCN2 and PKR, and phosphorylation of eIF2α at Ser 51 triggers the formation of SG (Anderson and Kedersha, 2008). Upon recognition of dsRNA by PKR, autophosphorylation of PKR occurs and the consequent hyperphosphorylated PKR catalyzes the phosphorylation of heterologous substrates (Dey et al., 2005) (Lu et al., 1999). Because DHX36 is required for avSG formation, I further evaluated the effect of DHX36 on PKR phosphorylation induced by viral infection or poly I:C transfection using DHX36 KO-inducible MEF or DHX36-depleted HEK293T cells. Viral infection (Fig. 22A) or poly I:C transfection (Fig. 22B) induced

phosphorylation of PKR. Interestingly, level of PKR phosphorylation was markedly attenuated in DHX36 KO cells (Fig. 22A and 22B). Transfection of poly I:C similarly induced the PKR phosphorylation in HEK293T cells (Fig. 22C). However, depletion of DHX36 diminished the PKR phosphorylation, suggesting that DHX36 is required for efficient activation of PKR induced by dsRNA.

2-13 ATPase activity of DHX36 is involved in the regulation of PKR activation

To further analyze the regulatory role of DHX36 in the activation of PKR, I transiently overexpressed HA-tagged DHX36 in HEK293T cells and evaluated the level of PKR phosphorylation in mock- or NDV-infected cells. While overexpression of DHX36 alone did not induce PKR phosphorylation (Fig. 23A, lane 1 and 2, and Fig. 23B), NDV-induced PKR phosphorylation was augmented by ectopic expression of DHX36 (Fig. 23A, lane 4 and 5, and Fig. 23B). Because DHX36 is a putative RNA ATPase/helicase, next I asked whether these catalytic activities are involved in PKR activation. To address this, the effect of ATPase-defective DHX36 mutant, E335A (Tran et al., 2004) on PKR phosphorylation was tested. Interestingly, ectopic expression of DHX36 E335A inhibited NDV-induced PKR phosphorylation presumably by its dominant negative effect, indicating that the

ATPase/Helicase activity is involved in PKR activation (Fig. 23A, lane 4-6, and Fig. 23B). Altogether, these data demonstrate that DHX36 augment the phosphorylation of PKR by viral infection and ATPase activity of DHX36 is involved in this regulation.

2-14 DHX36 augments the binding affinity of PKR to dsRNA

Since ATPase activity of DHX36 is involved in PKR activation by dsRNA, I further asked if the physical interaction between PKR and dsRNA is affected by the presence of DHX36. To address this, I performed pull-down assay using normal and DHX36-depleted cell lysates by pIC-conjugated beads and evaluated the level of antiviral proteins bound to the RNP complex. The association of RIG-I with pIC was not affected by absence of DHX36 (Fig. 24A and 24B, see RIG-I). However, the level of PKR that bound to dsRNA was moderately decreased with a concomitant reduction of phospho-PKR (Fig. 24A and 24B, see PKR and phospho PKR). Since total PKR amount was not affected by the absence of DHX36, these data suggest that DHX36 is capable of facilitating PKR association with dsRNA, hence its activation.

2-15 Expression and functional analysis of recombinant DHX36 and PKR

Although my data clearly showed that DHX36 augments PKR phosphorylation in a RNA ligand-dependent manner, it is still possible that other cellular factors might also contribute to PKR activation. Indeed, DHX36 forms a complex with other RNA helicases for innate immune responses induced by dsRNA (Zhang et al., 2011) (Fig. 16A). To clarify this issue, I further examined whether DHX36 directly facilitates PKR phosphorylation or requires other cofactors for PKR activation. To evaluate this, I performed an *in vitro* PKR phosphorylation assay using purified recombinant PKR, DHX36 WT and DHX36 E335A from the E. coli system. The level of expression and purification of the recombinant proteins were confirmed by SDS-PAGE gel staining (Fig. 25A). Next, I confirmed that purified recombinant DHX36 WT, but not E335A, retained the intrinsic ATPase activity by ATPase assay (Fig. 25B). The intrinsic kinase function of the recombinant PKR was also confirmed by in vitro phosphorylation analysis (Fig. 25C). Based on the data from Fig. 25C, the optimal condition of in vitro phosphorylation assay was determined and I chose 1 ng of pIC for further analysis.

2-16 DHX36 facilitates PKR phosphorylation

Using purified recombinant proteins (Fig. 25), I performed in vitro phosphorylation assay to confirm the direct effect of DHX36 on PKR activation in vitro. As shown in Fig. 26A, PKR

phosphorylation was detected by pIC treatment (Fig. 26A, lane 1 and lane 2). Intriguingly, the PKR phosphorylation was remarkably increased in the presence of DHX36 in a dose-dependent manner (Fig. 26A, lane 3-5). In contrast, the augmentation of PKR phosphorylation was not detected by DHX36 E335A (Fig. 26A, lane 6-8), confirming the involvement of ATPase activity in vitro. In addition, non-related control experiment using BSA showed no significant effect on PKR activation (Fig. 26A, lane 9-11). The level of input proteins for this analysis was confirmed by Western blot (Fig. 26A, lower panel) or silver staining (Fig. 26B). Taken together, these data indicate that DHX36 solely functions for efficient PKR activation in the presence of dsRNA through its ATPase activity.

2-17 DHX36 contributes to maximal antiviral effect

Type I IFN plays a fundamental role in protection against virus infection by suppressing viral yield and promoting cell survival. To conclusively determine if DHX36 exerts antiviral effects through its regulation of IFN induction, I used control WT or DHX36 KO- induced MEFs and evaluated cell viability as well as virus replication levels by NDV infection. Compared with control WT cells, severe cell death was observed in DHX36 KO-induced cells by NDV infection (Fig. 27A and 27B). Furthermore, NDV replication in DHX36 KO-induced cells was significantly increased compared to that in WT cells (Fig. 27C). Consistent with the

increased cytopathic effect and virus replication in DHX36 KO, enhanced viral titer (Fig. 27D) was observed in DHX36 KO, suggesting that DHX36 exerts its antiviral effect through the regulation of IFN production.

3. Discussion

The cytoplasmic viral RNA sensor, RLR, plays a major role in detecting viral infection and triggering antiviral responses. It has been suggested that multiple RNA helicases cooperatively promote their antiviral roles and contribute to innate immune responses (Fullam and Schroder, 2013). Moreover, it is suggested that contribution of RNA helicases to host antiviral responses might be variable by different cell types (Kato et al., 2005). In this report, I describe the involvement of DHX36 in sensing viral infection and subsequent IFN induction by RIG-I. Recent study suggested that DHX36 functions as DNA sensor and interacts with MyD88, an adaptor molecule in TLR-dependent signaling, in plasmacytoid dendritic cells (pDC) (Kim et al., 2010). Notably, the reported function of DHX36 is apparently distinct from our discovery. First, I tested the role of DHX36 using fibroblast and epithelial cell lines, quite distinct cell types from pDC in term of the antiviral sensing mechanism (Kim et al., 2010). Second, the stimuli used in my study did not contain or produce DNA. There is another study demonstrating the role of DHX36 as a dsRNA sensor in myeloid dendritic cells (mDC) (Zhang et al., 2011). DHX36 appears to function upstream of TRIF, another adaptor molecule in TLR-dependent signaling, to activate NF-κB and IRF-3/7. Again, their observation is distinct from my study because RIG-I was essentially involved in the antiviral signaling triggered by dsRNA, IAVΔNS1, and NDV in the fibroblast cells (Kato et al., 2006). It remains to be shown whether

dsRNA-stimulated mDC promotes PKR activation and SG formation through DHX36.

In this study, I observed that DHX36 augments RIG-I-mediated antiviral signaling in a stimulus-dependent manner by showing that signaling induced by infection with IAV∆NS1, NDV and transfection of pIC, but not 5'ppp 27, is enhanced by DHX36 (Fig. 10-11). Previously, we and others have shown that SG formation is required to facilitate antiviral responses of host cells (Ng et al., 2013) (Okonski and Samuel, 2013) (Onomoto et al., 2012) (Simpson-Holley et al., 2011). In fact, the majority of viruses reported, including Sindbis, encephalomyocarditis, polio, adeno-, and measles viruses induce SG upon infection (Ng et al., 2013) (Okonski and Samuel, 2013) (Onomoto et al., 2012) (White and Lloyd, 2012). Interestingly, I found that the augmentation of DHX36 for IFN signaling was only observed when cells were induced with stimuli that commonly trigger SG formation. In contrast, DHX36 was dispensable for the antiviral responses by stimulus that did not induce avSG. Moreover, the magnitude of IFN expression was much higher in avSG-dependent signal pathway compare to that induced without avSG (Fig. 10-11) and these results were consistent with my previous data (Fig. 5-7).

What is the underlying mechanism of DHX36 for this regulation?

I discovered that DHX36 mediates avSG formation by facilitating the activation of PKR in the presence of dsRNA (Fig. 22, Fig. 23 and Fig. 26, and also see a hypothetical model in Fig. 28). DHX36 was found to

physically interact with RIG-I regardless of virus infection (Fig. 14-15 and Fig. 17). Upon viral infection, DHX36:RIG-I complex recognizes dsRNA. PKR also binds to dsRNA and interacts with DHX36:RIG-I complex in a ligand-dependent manner (Fig. 14 and Fig. 16). Then, this complex further facilitates the efficient activation of PKR. It is clarified that DHX36 is capable of resolving several types of nucleotides containing unusual structures, such as G4-DNA and G4-RNA, and promotes further biological events (Booy et al., 2012) (Giri et al., 2011). Based on this notion, I speculated that DHX36 might modify RNA ligand through its intrinsic ATPase/helicase activity and serve an optimal ligand for better PKR recognition. Interestingly, depletion of DHX36 result in reduced PKR binding to dsRNA (Fig. 24). Furthermore, ATPase-deficient DHX36 did not affect PKR activation (Fig. 23 and Fig. 26), suggesting that ATP hydrolysis and/or dsRNA unwinding are mechanistically involved in this regulation. However, since augmentation of DHX36 for PKR binding affinity to dsRNA is modest, other unknown mechanism(s) might be involved in facilitating maximal PKR activation by DHX36. It is tempting to speculate that DHX36 changes conformation upon binding with dsRNA in the presence of ATP in a similar manner as another DExD/H box RNA helicase, RIG-I (Takahasi et al., 2008), to accelerate PKR activation with dsRNA. Finally, PKR activation subsequently induces avSG assembly and provides a platform of antiviral signal transduction by recruitment of TRIM25, a critical signaling molecule (Fig. 19).

Generally, replication of RNA viruses does not take place in soluble compartments. Viruses hijack host cell factors or create a *de novo* compartment to replicate, resulting in evasion from host sensing of foreign nucleic acids. Formation of avSGs may be one of the means to force viral nucleic acids to be exposed to host immune sensors and facilitate antiviral responses. This notion is consistent with the observations that avSGs facilitate immune sensing but is not an absolute requirement (Fig. 5 and Fig. 8).

Notably, PKR or DHX36 did not affect IFN-ß induction by 5'ppp 27 (Fig. 6 and Fig.10-11), even though this stimulus activates RIG-I (Kato et al., 2011). This is because 5'ppp 27 inadequately activates PKR and subsequent avSGs (Fig. 4-5 and Fig. 7). Since the amount of IFN induced by 5'ppp 27 is low (Fig. 5-7 and Fig 10), it remains to be explored if conferring PKR activation function to 5'ppp 27 results in enhanced signaling. Alternatively, 5'ppp 27 may bypass the requirement of avSG formation through an unknown mechanism(s). In this regard, it is tempting to hypothesize the existence of an adaptor molecule(s) that facilitates the activation of RIG-I with short 5'ppp 27 to signal without avSGs. This may be relevant to the previous observation that the 5'ppp moiety is essential for RIG-I to detect short dsRNA (<50 bp) but is dispensable for long dsRNA sensing (100-500 bp) (Hornung et al., 2006) (Kato et al., 2008). Indeed, my data showed that induction of IFN-ß and inflammatory cytokine by longer RNA (5'ppp 137) did not require 5'ppp moiety (Fig. 7), indicating the distinct

mechanisms on antiviral signaling, presumably through avSG-dependent and -independent pathway.

Altogether, in this study I describe a novel function of DHX36 in virus-induced SG formation through PKR activation. We have been proposing a model in which SG functions as a platform to facilitate viral dsRNA recognition and signal transduction by RLR (Onomoto et al., 2012). The results described here further support our model and emphasize the critical involvement of the virus-induced stress responses in antiviral innate immune responses.

Materials and Methods

Cell Culture and Transfection

HeLa and HEK293T cells were maintained in Dulbecco's modified Eagle's medium (DMEM) supplemented with 10% fetal bovine serum (FBS) and penicillin-streptomycin (100 U/ml and 100 μg/ml, respectively). DHX36 WT or KO-inducible MEFs (GFP or CRE-GFP), and DHX36 knockdown-inducible HeLa cells were kindly provided by Dr. Nagamine (Friedrich Miescher Institute for Biomedical Research, Basel, Switzerland) (Lai et al., 2012) (Iwamoto et al., 2008). Briefly, DHX36 KO was induced by treatment with 1 μM tamoxifen (Sigma-Aldrich, St Louis, MO) in the culture medium for 72 h and the DHX36 KO was confirmed by Western blot analysis. HeLa cell stably expressing GFP-G3BP1 (GFP-G3BP1 HeLa) was previously reported by our group (Ng et al., 2013). The GFP-tagged-DHX36 constructs (GFP-DHX36 WT, GFP-DHX36 N-term, GFP-DHX36 Helicase, and GFP-DHX36 C-term) were kindly provided by Dr. Nagamine (Chalupnikova et al., 2008). The pEF-Bos-HA-DHX36 was constructed by inserting the PCR-amplified full-length DHX36 coding sequences from GFP-DHX36 WT between *Bgl*II and *BamH*I sites of pEF-Bos vector. The pEF-Bos-HA-DHX36 E335A was constructed with a KOD-Plus-Mutagenesis kit (Toyobo, Osaka, Japan) using the pEF-Bos-HA-DHX36 as a template. pBos-FLAG-RIG-I WT (RIG-I 1-925) and pBos-FLAG-RIG-IΔCTD (RIG-I 1-801) were described previously (Kageyama et al., 2011). All constructs were transfected into HEK293T cells with

Lipofectamine 2000 (Invitrogen, Carlsbad, CA) for the experiments.

RNA Transfection and Virus Infection

Poly I:C was purchased from Amersham Biosciences (Arlington Heights, IL). 5'ppp RNAs were synthesized by *in vitro* transcription using the AmpliScribe T7-Flash Transcription kit (Epicentre, Madison, WI). RNAs were delivered into the cells with Lipofectamine 2000 according to the manufacturer's instructions. Influenza A virus ΔNS1 strain (A/PR/8/34, ΔNS1) was originally produced by Dr. A. Garcia-Sastre (Mount Sinai School of Medicine, USA), and provided by Dr. S. Akira (Osaka University, Japan). Newcastle disease virus (Miyadera strain) was provided by Dr. Taniguchi (University of Tokyo, Japan). For virus infection, cells were washed with PBS and treated with the culture medium ('mock-treated') or infected with IAVΔNS1 or NDV in serum-free and antibiotic-free medium. After adsorption at 37°C for 1 h, the medium was changed and infection was continued for various periods in the presence of serum-containing DMEM.

Poly I:C Pull down, Immunoprecipitation, and Antibodies.

Poly I:C pull down assay was performed as described previously (Yoneyama et al., 2004). Stable transformants of FLAG-RIG-I in *rig-i* null MEFs (RIG-I null/FLAG-RIG-I) were established by transfection of a linearized plasmid (pBos-FLAG-RIG-I WT) (Kageyama et al., 2011), and selected with Puromycin. Immunoprecipitation was performed

using whole-cell extracts from HeLa, HEK293T, GFP-G3BP1 HeLa, or RIG-I null/FLAG-RIG-I cells (200 μg), together with 1 μg anti-FLAG (Sigma-Aldrich, St. Luis, MO, F3165), or anti-GFP (Wako, Osaka, Japan, mFX73) antibodies. After overnight incubation at 4°C, immune complexes were precipitated with protein A-sepharose beads (Amersham Biosciences) and analyzed by SDS-PAGE and Western blotting. Anti-human and -mouse IRF-3 polyclonal antibody, and anti-RIG-I polyclonal antibody were previously described (Onomoto et al., 2012) (Iwamura et al., 2001). Anti-human DHX36 monoclonal antibody was kindly provided by Dr. Nagamine (Iwamoto et al., 2008). The monoclonal antibody against Influenza NP (mAb61A5) was generated by Dr. Y. Kikuch (Iwaki Meisei University, Japan), and provided by Dr. F. Momose (Kitasato University, Japan) (Momose et al., 2007). The anti-NDV NP monoclonal antibody was produced by Dr. Y. Nagai, and provided by Dr. T. Sakaguchi (Hiroshima University, Japan). Other antibodies used in this study were as follows: anti-phospho PKR T451 (Abcam, ab4818), anti-G3BP (Santa Cruz, sc-70283), anti-TIAR (Santa Cruz, sc-1749), anti-Actin (Sigma-Aldrich, A-1978), and anti-TRIM25 (Santa Cruz, sc-22832) antibodies. For immunofluorescence analysis, Alexa 488-, 594-, and 633- conjugated anti-mouse, anti-rabbit, or anti-goat IgG antibodies purchased from Invitrogen were used as secondary antibodies. Propidium Iodide (PI) (1:2,000 in PBST) (Miltenyi Biotec) was used for cytoplasmic dsRNA staining.

Poly I:C Binding Assay

RNA binding assay was previously reported (Takahasi et al., 2008). Briefly, recombinant DHX36 (1.5 μg) was mixed with 1 μg of pIC in total 10 μl of DHX36 buffer [50 mM Tris pH 7.5, 50 mM KCl, 5 mM DTT, 20% (v/v) glycerol] and incubated at 25°C for 15 min. Then, the mixture was applied to 1% agarose gel and stained with ethidium bromide (EtBr).

RNA-Immunoprecipitation (RIP) Assay

RIP assay was performed using cell extracts from mock- or IAVΔNS1-infected HeLa cells with anti-human DHX36 monoclonal antibody by RiboCluster Profiler RIP-Assay Kit (MBL, Japan, RN1001) according to the manufacturer's recommendations. Briefly, RNA-protein complex was pulled-down with 5 μg of mouse normal IgG (Santa Cruz, sc-2025) or anti-DHX36 monoclonal antibody. Then, bound RNAs were recovered from the RNA-protein complex and used for cDNA synthesis. Real-time qPCR was further performed to evaluate the RNA level bound to DHX36 with the specific primer sets targeting IAV gene. As an internal control, human glyceraldehyde 3-phosphate dehydrogenase (GAPDH) gene was targeted. Sequence information of primers is as follows: IAV segment 5, 5'-GATGGAGACTGATGGAGAACGCCAG-3' (Sense), 5'-AGCTGTTTTGGATCAACCGTCCCTC-3' (antisense); IAV segment 6, 5'-GGACAGAGACTGATAGTAAG-3' (sense), 5'-GTTAGCTCAGGATGTTGAAC-3' (antisense); IAV segment 8, 5'-GATAACACAGTTCGAGTCTC-3' (sense), 5'-

TTTCTCGTTTCTGTTTTGGA-3' (antisense); human GAPDH, 5'-ACTGCCAACGTGTCAGTGGT-3' (sense), 5'-TTACTCCTTGGAGGCCATGT-3' (antisense).

Enzyme-linked Immunosorbent Assay (ELISA)

Culture supernatants were collected and subjected to ELISA with mouse IFN-ß kit (PBL Interferon Source, Piscataway, NJ) according to the manufacturer's instructions.

Quantitative Reverse-Transcription PCR

Quantitative reverse transcription-PCR for IFN-ß was performed as described previously (Onomoto et al., 2012). TaqMan probe for human IL-8 was purchased from Applied Biosystems. For the evaluation of viral RNA, quantitative reverse-transcription PCR was performed using SYBR green reagent (Applied Biosystems, CA, USA, 4385612) with the specific primer sets targeting NDV (F and N) or IAV (segment 5, 6 and 8) genes. As an internal control, human and mouse GAPDH gene was targeted and amplified. Sequence information of primers is as follows: NDV F, 5'-GCAGCTGCAGGGATTGTGGT-3' (sense), 5'-TCTTTGAGCAGGAGGATGTTG-3' (antisense); NDV N, 5'-CTCAAGAGAGGCCGCAATAC-3' (sense), 5'-AGTGCAAGGGCTGATGTCTT-3' (antisense); mouse GAPDH, 5'-ATCTTCTTGTGCAGTGCCAGCCTCGTCCCG-3' (sense), 5'-AGTTGAGGTCAATGAAGGGGTCGTTGATGG-3' (antisense).

Sequence information of human GAPDH is described above.

Immunofluorescence Microscopy and Fluorescence Live Imaging

Virus-infected HeLa or GFP-G3BP1 HeLa cells were fixed with 4% paraformaldehyde (PFA) for 20 min at 4°C, permeabilized with 0.05% Triton X-100 in PBS for 5 min at room temperature (RT), blocked with 5 mg/ml BSA in PBST (0.04% Tween20 in PBS) for 30 min, and incubated at 4°C overnight with the relevant primary antibodies diluted in blocking buffer. The cells were then incubated with secondary antibodies at room temperature for 1 h. Nuclei were stained with 4.6-dimaidino-2-phenylinodole (DAPI) and analyzed with a confocal laser microscope, TCS-SP (Leica).

For fluorescence live imaging, GFP-G3BP1 HeLa cells were stimulated by either NDV infection or RNA ligand transfection as described above. After 12 h stimulation, GFP fluorescence images were taken and analyzed with a fluorescence microscope system, AF6500 (Leica). The percentages of avSG-containing cells were calculated in more than five randomly chosen fields for each slide.

RNA Interference

The siRNA negative control (Invitrogen, Cat. No. 1293-112) and siRNAs targeting human PKR (sense: 5'-UUUACUUCACGCUCCGCCUUCUCGU-3', antisense: 5'-ACGAGAAGGCGGAGCGUGAAGUAAA-3') and DHX36 (sense: 5'-

UUCUACUGCUUACAAAUCCAGCUCC-3', antisense: 5'-GGAGCUGGAUUUGUAAGCAGUAGAA-3') were purchased from Invitrogen, and the siRNAs targeting human RIG-I (sense: 5'-CGGAUUAGCGACAAAUUUAUU-3', antisense: 5'-UAAAUUUGUCGCUAAUCCGUU-3') and mouse DHX36 (sense: 5'-CUACAACUGGCUUAUCUAUUU-3', antisense: 5'-AUAGAUAAGCCAGUUGUAGUU-3') were purchased from Genolution Pharmaceutical (Seoul, Korea). For knock down of target genes, siRNAs were transfected into the cells with RNAi MAX (Invitrogen) according to the manufacturer's recommendations. At 48 h or 72 h post-transfection, cells were harvested or infected with viruses for further experiments.

Expression and Purification of Recombinant Protein

pEGST-PKR/λPP plasmid that encodes GST-fused PKR and λ protein phosphatase was kindly gifted from Dr. Takayasu Date (Kanazawa Medical University). The vector was transformed into *E. Coli* BL21(DE3)pLysS strain. The Bacteria was first grown at 37°C in LB medium containing 100 mg/ml ampicillin. Protein expression was induced by addition of 1 mM IPTG when the absorbance at 600 nm was approximately 0.4. The cells were then grown at 25°C for 16 h. After incubation, the cells were harvested by centrifugation and resuspended in PBS supplemented with protease inhibitor cocktail (EDTA free) (nacalai tesuque) and was lysed via sonication. The

supernatant was collected by centrifugation and mixed with Glutathione Sepharose 4B (GE Healthcare) for 3hr at 4°C. The protein bound to Glutathione Sepharose 4B was washed with PBS and further washed with PBS supplemented with 500 mM NaCl to remove the *E. Coli* derived nucleic acid from GST-PKR. Then the protein was eluted by elution buffer containing 50 mM Tris pH 7.5, 50 mM KCl, 5 mM DTT, 20% (v/v) glycerol, 10 mM Glutathione and was concentrated. The purity of PKR was estimated by the Gelanalyzer program (http://www.gelanalyzer.com/) and approximate purity was 80 %. No contamination of *E. Coli* derived nucleic acid was confirmed by UV spectrometer.

To obtain the purified recombinant DHX36 WT and its ATPase-dead mutant, E335A, the intact human DHX36 and E335A were amplified by PCR and inserted into a pEt22b(+) (Novagen) to produce a C-terminally hexa-histidine tagged protein. The vector was transformed into *E. Coli* BL21(DE3) strain. The Bacteria was similarly grown at 37°C in LB medium containing 100 mg/ml ampicillin. The protein expression was induced by the addition of 0.01 mM IPTG when the absorbance at 600 nm was approximately 0.4. Then the cells were grown at 16°C for 16 h. The cells were harvested by centrifugation and suspended in lysis buffer containing 50 mM Tris pH8 500 mM NaCl, 20 mM Imidazole supplemented with protease inhibitor cocktail and were lysed via sonication and centrifuged. The supernatant was suspended with a Ni-NTA (Qiagen) affinity column, then the resin was washed with lysis

buffer. The protein was eluted with a gradient of 20-500 mM Imidazole dissolved in lysis buffer. The buffer containing the protein was exchanged to 50 mM Tris pH 7.5, 50 mM KCl, 5 mM DTT, 20% (v/v) glycerol and concentrated. The purity of proteins was further confirmed and approximate purity was 80 %. No contamination of *E. Coli* derived nucleic acid was confirmed by UV spectrometer.

In vitro PKR Phosphorylation

In vitro PKR phosphorylation was determined in a total volume of 10 μl containing 50 mM Tris–HCl (pH 7.5), 2 mM $MgCl_2$, 50 mM KCl, 1 μg of purified GST-PKR (Matsui et al., 2001), and the indicated amounts of WT or E335A hexa-histidine-DHX36 and pIC. After incubation at 30 °C for 5 min, 1 μl of 10 mM ATP was supplemented and the reaction mixtures were further incubated at 30 °C for 15 min. The reaction was stopped by adding 10 μl of 2x SDS sample buffer and boiled for 5 min. Samples were subjected to SDS-PAGE and the level of phosphorylated PKR was evaluated by Western blot analysis using anti-phospho PKR specific antibody. Total amount of input protein level was also confirmed by silver staining.

ATPase Assay

0.35 mg of recombinant DHX36 WT or E335A was mock-treated or mixed with 0.25 μg pIC in a total volume of 20 μl buffer containing 20 mM Tris (pH 8.0), 1.5 mM $MgCl_2$, and 1.5 mM DTT and the mixture

was incubated at room temperature for 15 min. After incubation, 5 μl of 5 mM ATP was added and the mixture was further incubated at 37°C for 30 min. Finally, 5 μl of the mixture from the incubated samples was taken and diluted with 45 μl water, and 100 μl BIOMOL Green (Enzo life sciences, Farmingdale, NY) solution was added to the mixture. ATPase activity was examined by measuring the absorbance of 630 nm of the samples using a Microplate Reader 680 (Bio Rad).

Plaque Assay

DHX36 WT and KO MEF were infected with NDV for 24 h and culture supernatant was collected. Then, virus yield in culture supernatant was determined using Hep2 cells as previously described (Yoneyama et al., 2004).

Figure Legends

Figure 1. Schematic diagram of RLRs

The conserved domain of CARDs, DExH/D box RNA helicase domain and CTD of RLRs is shown. The critical site for ATPase activity is indicated by an asterisk.

Figure 2. RLR signal pathway

Upon viral infection, non-self RNAs such as 5'ppp secondary structured RNA or dsRNA, are recognized by host cytoplasmic sensors, RLRs and PKR. Recognition of RNA ligands induces conformational changes of RLR and PKR then both sensors become active signaling molecules. IFN signaling is propagated by CARD-CARD interaction between RLRs and IPS-1that is positively regulated by ubiquitination, which results in aggregation of RLRs and IPS-1. On the other side, activated PKR rapidly induces antiviral cytoplasmic stress granules, called avSG and provides a critical platform for RLR signaling, where antiviral proteins and signal molecules interacting. By forming avSG, IFN signaling is enhanced, however IFN signaling is still induced in avSG-independent manner. Finally, kinase complexes (TBK1 & IKKi)-induced IRF3 phosphorylation initiates the transcription of type I IFN gene.

Figure 3. PKR regulates avSG formation and IFN signaling induced by dsRNA

(A) GFP-G3BP1 HeLa cells were mock-treated or transfected with poly

I:C. After 12 h incubation, cells were lysed and subjected to Western blot with indicated antibodies.

(B-C) GFP-G3BP1 HeLa cells were transfected with control siRNA or siRNA targeting human PKR. After 48 hr incubation, cells were mock-treated or transfected with poly I:C for 9 h. dsRNA-induced SG formation or induction of IFN-β mRNA was examined by fluorescence microscopy (B) or real-time RT-PCR.

Figure 4. RNA length-dependent induction of antiviral protein expression

(A) Sequence information of ivt-RNAs.

(B) The quality of ivt-RNA was confirmed by EtBr staining (EtBr staining). HeLa cells were mock-treated or transfected with ivt-RNAs (5'ppp 27, 86 and 136) for 9 h. Then, cells were lysed and subjected to Western blot analysis using indicated antibodies (Western blot) to examine the level of antiviral proteins.

Figure 5. avSG enhances the expression of IFN-β and cytokine

(A-B) GFP-G3BP1 HeLa was mock-treated or transfected with indicated ivt-RNAs. After 9 h incubation, ivt-RNA-induced SG formation was monitored by fluorescence microscopy (A), and mRNA level of IFN-β and IL-8 was examined by real-time RT-PCR (B).

(C-D) HeLa cells stably expressing FLAG-RIG-I were mock-treated or transfected with indicated ivt-RNAs. After 9 h incubation, level of IRF3-

dimer (C) or RIG-I-oligomer (D) was evaluated by Native-PAGE analysis.

Figure 6. PKR regulates IFN signaling in a ligand-dependent manner

(A-B) HeLa cells were transfected with control siRNA or siRNA targeting human PKR. After 48 hr incubation, cells were mock-treated or transfected with indicated ivt-RNAs for 9 h. Then, cells were lysed and subjected to Native-PAGE to evaluate the IRF3 dimerization (A). The quantified IRF3 dimer level was shown in a bar graph (B).

Figure 7. 5'ppp is not required for avSG-mediated antiviral signaling

(A-B) GFP-G3BP1 HeLa was mock-treated or transfected with normal- or CIAP-treated ivt-RNAs. After 9 h incubation, ivt-RNA-induced SG formation was monitored by fluorescence microscopy (A), and mRNA induction of IFN-β and IL-8 was examined by real-time RT-PCR (B).

Figure 8. Hypothetical model

Upon viral infection, cytoplasmic antiviral sensors, RIG-I and PKR recognize non-self RNAs (5'ppp secondary structured RNA or dsRNA). Short 5'ppp RNA activates RIG-I signaling without avSG formation. The strength of IFN signaling is relatively weak (avSG-independent). In contrast, long 5'ppp RNA and dsRNA are recognized by RIG-I and PKR.

Upon PKR activation, avSG was formed and provide a place for antiviral protein interaction that facilitates oligomerization of RIG-I. Strong IFN signaling is occurred by PKR:avSG-dependent pathway (avSG-dependent).

Figure 9. Confirmation of DHX36 level in DHX36 WT or KO-inducible MEF

DHX36 WT (GFP) control or KO-inducible (Cre-GFP) MEF cells were mock-treated or treated with 1 μM of tamoxifen (OH-T). After incubation for indicated time, cells were lysed and subjected to Western blot to confirm the level of DHX36.

Figure 10. DHX36 regulates production of IFN-β in a stimulus-dependent manner

(A-D) DHX36 WT or KO-induced MEF cells were infected with IAVΔNS1 (A), NDV (B) or transfected with poly I:C (pIC) (C) or 5'ppp 27 (5'ppp) (D) as indicated. After 16 h infection or transfection, culture media were subjected to ELISA to determine IFN-ß protein level. Viruses: IAVΔNS1, Influenza virus with NS1 gene deletion; NDV, Newcastle disease virus. Data are the mean ± standard error of the mean (SEM), P value by Student's t test is indicated.

Figure 11. DHX36 regulates induction of IFN-β mRNA in a stimulus-dependent manner

(A-D) DHX36 WT or KO-induced MEF cells were infected with NDV (A and B) or transfected with poly I:C (pIC) (C) or 5'ppp 27 (5'ppp) (D) as indicated. After 9 h infection or transfection, cells were harvested and total RNA was collected. Level of NDV replication (B) and IFN-ß gene induction (A, C and D) was evaluated by real-time qPCR.
Viruses: IAVΔNS1, Influenza virus with NS1 gene deletion; NDV, Newcastle disease virus. Data are the mean ± standard error of the mean (SEM), P value by Student's t test is indicated.

Figure 12. DHX36 regulates IFN signaling through IRF3 activation

(A) DHX36 WT or KO cells were mock-treated, NDV-infected, or 5'ppp-transfected. After 9 h incubation, cells were subjected to native-PAGE and IRF-3 dimer was detected by immunoblotting using anti-mouse IRF-3 antibody.
(B and C) HEK293T cells was transfected with control siRNA or siRNA targeting human DHX36. After 48 h incubation, cells were mock-treated or infected with NDV. Whole-cell lysates at the indicated times were subjected to either Native-PAGE to examine the level of IRF-3 dimerization or SDS-PAGE to evaluate the protein level of DHX36 and actin by Western blot analysis (B). Level of NDV replication was confirmed by real-time RT-PCR (C).

Figure 13. DHX36 localizes in the stress granules with antiviral proteins by virus infection

(A-C) HeLa cells were mock-treated or infected with IAVΔNS1 for 12 h. Then, cells were fixed and stained for the proteins using indicated antibodies and localization of protein was analyzed by confocal microscopy. Nuclei were visualized by DAPI staining. High magnification images of the square area are represented (Enlarged). Cells with foci containing RIG-I, IAV NP, and TIAR were counted (A). Cells with foci containing DHX36 and TIAR or DHX36 and RIG-I were counted (B). Foci with PKR and TIAR or PKR and RIG-I were counted (C). Data are the mean standard ± error of the mean (SEM). (N.D = not detected).

Figure 14. DHX36 interacts with antiviral proteins

(A) HEK293T cells were transfected with empty vector, expression vector for Flag-tagged RIG-I WT, or Flag-tagged RIG-IΔCTD. After 24 h incubation, cells were mock treated or infected with IAVΔNS1 for 12 h. Whole-cell lysates (WCL) were prepared and immunoprecipitated with anti-Flag antibody. The precipitates (IP with Flag) were analyzed for DHX36 and PKR by immunoblotting. Input protein used for this experiment was confirmed (WCL).

(B) Total cell lysate from *rig-I* null or Flag-RIG-I stably expressing *rig-I* null MEFs were prepared and immunoprecipitated with anti-Flag antibody. The precipitates (IP: Flag) were analyzed for mouse DHX36 and Flag by SDS-PAGE. Protein expression in the whole-cell lysate (WCL) was confirmed by immunoblotting.

Figure 15. DHX36 interacts with RIG-I through its helicase domain

(A) HEK293T cells were transfected with empty vector or expression vector for GFP-tagged DHX36 WT or GFP-tagged DHX36 deletion mutants together with Flag-tagged RIG-I as indicated. After 24 h incubation, whole-cell lysates (WCL) were prepared and immunoprecipitated with anti-Flag antibody. The precipitates (IP: Flag) were analyzed for DHX36 (IB: GFP) and RIG-I (IB: Flag) by immunoblotting. Input protein used for this experiment was confirmed (WCL).

* and ** represent the 'non-specific' and 'IgG' bands, respectively.

Figure 16. DHX36 forms a complex with antiviral proteins and dsRNA

(A) Total cell lysate from uninfected HeLa cells was precipitated with either empty (Beads) or poly I:C-conjugated beads (pIC-Beads) in the presence of RNase inhibitor. The precipitates were further subjected to Western blotting to evaluate the protein-dsRNA interaction using the indicated antibodies.

(B) Recombinant DHX36 (1.5 μg) was mixed with poly I:C (1 μg) and separated on 1 % agarose gel by electrophresis. The gel was stained with ethidium bromide (EtBr) and visualized by ultra violet illumination.

Figure 17. DHX36 recognizes IAV RNA

(A-C) HeLa cells were mock-treated or infected with IAV∆NS1. After 12 h infection, cells were harvested and lysed for RNA-IP analysis. After pull-down with indicated antibodies, RNA was recovered from the RNP complex. The IP efficiency was confirmed by Western blot analysis by indicated antibodies (A). The level of RNAs bound to RNP complex as well as input RNAs was measured by real-time RT-PCR with indicated probes (B). DHX36 affinity to RNAs was examined by calculating the ratio of RNAs from DHX36 IP and IgG IP (C).

Figure 18. DHX36 and RIG-I co-localize with IAV RNA

HeLa cells were mock-treated or infected with IAV∆NS1. After 12 h infection, cells were fixed and stained for the indicated proteins. Cytoplasmic dsRNAs were detected by PI staining. Nuclei were visualized by DAPI staining. The localization between proteins and dsRNAs were analyzed by confocal microscopy. High magnification images of the square area are represented (Enlarged).

Figure 19. TRIM25 co-localizes with avSG by virus infection or dsRNA transfection

(A) GFP-G3BP1 HeLa cells were mock-treated or infected with viruses or transfected with pIC as indicated. After 12 h incubation, cells were fixed and stained for DHX36 and TRIM25. GFP-G3BP1 was detected by fluorescence. Nuclei were visualized by DAPI staining. The images were taken by confocal microscopy. High magnification images of the

square area are shown (Enlarged).

(B) HeLa cells were mock-treated or treated with 0.5 mM of sodium arsenite for 45 min. After stimulation, cells were fixed and stained for the indicated proteins. Nuclei were visualized by DAPI staining. The images were taken by confocal microscopy. High magnification images of the square area are shown (Enlarged).

(C) HeLa cells were mock-treated or stimulated with indicated stimuli. After incubation for 12 h for virus infection or pIC transfection, or for 45 min for sodium arsenite, cells were collected and total RNA was isolated. Level of IFN-ß gene induction was examined by real-time RT-PCR. Data are the mean ± standard error of the mean (SEM).

Figure 20. DHX36 mediates avSG formation

(A) HeLa cells were transfected with control siRNA or siRNA targeting for human DHX36. After 48 h incubation, cells were infected with IAV∆NS1 for 12 h. Then, cells were fixed and stained for IRF-3, IAV NP and TIAR. The percentage of cells showing cytoplasmic TIAR foci and nuclear IRF-3 was determined by cell counting (bar graph).

(B) GFP-G3BP1 HeLa cells were transfected with control siRNA or siRNA targeting human DHX36 for 72 h. The cells were mock-treated or infected with NDV for indicated times. Cellular localization of GFP-G3BP1 was examined by florescent microscopy and GFP foci were quantified and shown in a graph.

Figure 21. DHX36 affects interaction between RIG-I and G3BP1

GFP-G3BP1 HeLa cells were transfected with control siRNA or siRNA targeting for human DHX36. After 72 h incubation, cells were infected with NDV for 12 h and total cell lysates were immunoprecipitated with either control IgG or anti-GFP antibody. Immunoprecipitates (IP) were analyzed by Western blotting with indicated antibodies. Input proteins used for this experiment was confirmed by immunoblotting using whole-cell lysate (WCL).

Figure 22. DHX36 facilitates PKR phosphorylation by virus infection or dsRNA transfection

(A and B) Tamoxifen-induced control (WT) and DHX36 knockout (KO) MEF cells were mock-treated or infected with indicated viruses (A) or transfected with poly I:C (B). After 12 h incubation, cells were lysed and protein level was examined by Western blotting using indicated antibodies.

(C) HEK293T cells were transfected with control siRNA or siRNA targeting for human DHX36. After 72 hr incubation, cells were induced by poly I:C transfection for the indicated times. Total cell lysates were prepared and protein level was examined by Western blotting using indicated antibodies.

Figure 23. ATPase activity of DHX36 is involved in the regulation of PKR activation

(A and B) HEK293T cells were transfected with empty vector, expression vector for HA-DHX36, or HA-DHX36 E335A. After 24 h incubation, cells were mock-treated or infected with NDV for 12 h. Then, cells were collected and analyzed for the level of indicated proteins by immunoblotting (A). Quantification of the signals for phospho-PKR is shown (B).

Figure 24. DHX36 affects the binding affinity of PKR to dsRNA

(A and B) HeLa cells were transfected with control siRNA or that targeting human DHX36. After 72 h incubation, cells were collected and total cell lysates were pulled down with empty- (Beads) or poly I:C-Beads (pIC-Beads). The precipitated proteins (Pull down) were analyzed by immunoblotting using the indicated antibodies. Input proteins utilized for this experiment were confirmed by immunoblotting (WCL) (A). Quantification of the signals for RIG-I, PKR or phospho-PKR is represented in the bar graphs (B).

Figure 25. Expression and functional analysis of recombinant DHX36 and PKR

(A) The purity of recombinant proteins were confirmed by SDS-PAGE and gel staining with coomassie blue.

(B) Functional activity of recombinant DHX36 WT and E335A was confirmed by ATPase assay using poly I:C.

(C) PKR autophosphorylation analysis was performed with poly I:C to

confirm the functional activity of recombinant PKR. Both normal and phosphorylated PKR were examined by Western blotting using indicated antibodies.

Figure 26. DHX36 facilitates PKR phosphorylation

(A) PKR autophosphorylation analysis was performed with poly I:C and recombinant WT or E335A DHX36 as indicated. The level of proteins was analyzed by Western blotting using indicated antibodies.
(B) Input proteins used for in this experiment were confirmed by standard silver staining. The size of each protein is indicated by arrowhead.

Figure 27. DHX36 exerts its antiviral activity

(A) Tamoxifen-induced control (WT) and DHX36 knockout (KO) cells were mock-treated or infected with NDV for 24 h. Microscopic morphology of the cells (A) and amido black stained culture dish (B) are shown. Yield of viral RNAs after 18 h infection was examined by real-time RT-PCR using indicated probes (C). Yield of infectious viral particles were measured by plaque assay using culture supernatant from NDV infected (24 h) DHX36 WT or KO-induced MEF (D).
Data are the mean ± standard error of the mean (SEM), P value by Student's t test is indicated.

Figure 28. Hypothetical model of DHX36 augmentation for RIG-I

signaling

DHX36 and RIG-I physically interact regardless of viral infection (I. Normal state). Upon viral infection, dsRNA facilitates formation of RIG-I/DHX36/PKR/dsRNA complex. DHX36 moderately increase the affinity of PKR for dsRNAs sensing as well as promoting activation of PKR through its ATPase activity (II. PAMP recognition). Finally, the activated PKR immediately induces avSG and provides a critical platform for host antiviral responses by recruitment of antiviral signal molecule, TRIM25 (III. Signal transduction).

References

Ablasser, A., Bauernfeind, F., Hartmann, G., Latz, E., Fitzgerald, K.A., and Hornung, V. (2009). RIG-I-dependent sensing of poly(dA:dT) through the induction of an RNA polymerase III-transcribed RNA intermediate. Nature immunology *10*, 1065-1072.

Anderson, P., and Kedersha, N. (2002). Visibly stressed: the role of eIF2, TIA-1, and stress granules in protein translation. Cell stress & chaperones *7*, 213-221.

Anderson, P., and Kedersha, N. (2008). Stress granules: the Tao of RNA triage. Trends in biochemical sciences *33*, 141-150.

Ariumi, Y., Kuroki, M., Kushima, Y., Osugi, K., Hijikata, M., Maki, M., Ikeda, M., and Kato, N. (2011). Hepatitis C virus hijacks P-body and stress granule components around lipid droplets. Journal of virology *85*, 6882-6892.

Balachandran, S., and Barber, G.N. (2007). PKR in innate immunity, cancer, and viral oncolysis. Methods in molecular biology *383*, 277-301.

Baum, A., and Garcia-Sastre, A. (2011). Differential recognition of viral RNA by RIG-I. Virulence *2*, 166-169.

Booy, E.P., Meier, M., Okun, N., Novakowski, S.K., Xiong, S., Stetefeld, J., and McKenna, S.A. (2012). The RNA helicase RHAU (DHX36) unwinds a G4-quadruplex in human telomerase RNA and promotes the formation of the P1 helix template boundary. Nucleic acids research *40*, 4110-4124.

Carroll, K., Hastings, C., and Miller, C.L. (2014). Amino acids 78 and 79 of Mammalian Orthoreovirus protein microNS are necessary for stress granule

localization, core protein lambda2 interaction, and de novo virus replication. Virology *448*, 133-145.

Chalupnikova, K., Lattmann, S., Selak, N., Iwamoto, F., Fujiki, Y., and Nagamine, Y. (2008). Recruitment of the RNA helicase RHAU to stress granules via a unique RNA-binding domain. The Journal of biological chemistry *283*, 35186-35198.

Chen, G., Shaw, M.H., Kim, Y.G., and Nunez, G. (2009). NOD-like receptors: role in innate immunity and inflammatory disease. Annu Rev Pathol *4*, 365-398.

Chiu, Y.H., Macmillan, J.B., and Chen, Z.J. (2009). RNA polymerase III detects cytosolic DNA and induces type I interferons through the RIG-I pathway. Cell *138*, 576-591.

Creacy, S.D., Routh, E.D., Iwamoto, F., Nagamine, Y., Akman, S.A., and Vaughn, J.P. (2008). G4 resolvase 1 binds both DNA and RNA tetramolecular quadruplex with high affinity and is the major source of tetramolecular quadruplex G4-DNA and G4-RNA resolving activity in HeLa cell lysates. The Journal of biological chemistry *283*, 34626-34634.

Cuddihy, A.R., Wong, A.H., Tam, N.W., Li, S., and Koromilas, A.E. (1999). The double-stranded RNA activated protein kinase PKR physically associates with the tumor suppressor p53 protein and phosphorylates human p53 on serine 392 in vitro. Oncogene *18*, 2690-2702.

Cui, S., Eisenacher, K., Kirchhofer, A., Brzozka, K., Lammens, A., Lammens, K., Fujita, T., Conzelmann, K.K., Krug, A., and Hopfner, K.P. (2008). The C-

terminal regulatory domain is the RNA 5'-triphosphate sensor of RIG-I. Molecular cell *29*, 169-179.

Davis, W.G., Bowzard, J.B., Sharma, S.D., Wiens, M.E., Ranjan, P., Gangappa, S., Stuchlik, O., Pohl, J., Donis, R.O., Katz, J.M.*, et al.* (2012). The 3' untranslated regions of influenza genomic sequences are 5'PPP-independent ligands for RIG-I. PloS one *7*, e32661.

Dey, M., Cao, C., Dar, A.C., Tamura, T., Ozato, K., Sicheri, F., and Dever, T.E. (2005). Mechanistic link between PKR dimerization, autophosphorylation, and eIF2alpha substrate recognition. Cell *122*, 901-913.

Feng, Q., Hato, S.V., Langereis, M.A., Zoll, J., Virgen-Slane, R., Peisley, A., Hur, S., Semler, B.L., van Rij, R.P., and van Kuppeveld, F.J. (2012). MDA5 detects the double-stranded RNA replicative form in picornavirus-infected cells. Cell reports *2*, 1187-1196.

Fujita, T. (2009). A nonself RNA pattern: tri-p to panhandle. Immunity *31*, 4-5.

Fullam, A., and Schroder, M. (2013). DExD/H-box RNA helicases as mediators of anti-viral innate immunity and essential host factors for viral replication. Biochimica et biophysica acta *1829*, 854-865.

Fung, G., Ng, C.S., Zhang, J., Shi, J., Wong, J., Piesik, P., Han, L., Chu, F., Jagdeo, J., Jan, E.*, et al.* (2013). Production of a dominant-negative fragment due to G3BP1 cleavage contributes to the disruption of mitochondria-associated protective stress granules during CVB3 infection. PloS one *8*, e79546.

Gack, M.U., Shin, Y.C., Joo, C.H., Urano, T., Liang, C., Sun, L., Takeuchi, O., Akira, S., Chen, Z., Inoue, S.*, et al.* (2007). TRIM25 RING-finger E3 ubiquitin ligase is essential for RIG-I-mediated antiviral activity. Nature *446*, 916-920.

Garcia, M.A., Collado, M., Munoz-Fontela, C., Matheu, A., Marcos-Villar, L., Arroyo, J., Esteban, M., Serrano, M., and Rivas, C. (2006). Antiviral action of the tumor suppressor ARF. The EMBO journal *25*, 4284-4292.

Gilfoy, F.D., and Mason, P.W. (2007). West Nile virus-induced interferon production is mediated by the double-stranded RNA-dependent protein kinase PKR. Journal of virology *81*, 11148-11158.

Giri, B., Smaldino, P.J., Thys, R.G., Creacy, S.D., Routh, E.D., Hantgan, R.R., Lattmann, S., Nagamine, Y., Akman, S.A., and Vaughn, J.P. (2011). G4 resolvase 1 tightly binds and unwinds unimolecular G4-DNA. Nucleic acids research *39*, 7161-7178.

Goh, K.C., deVeer, M.J., and Williams, B.R. (2000). The protein kinase PKR is required for p38 MAPK activation and the innate immune response to bacterial endotoxin. The EMBO journal *19*, 4292-4297.

Hornung, V., Ellegast, J., Kim, S., Brzozka, K., Jung, A., Kato, H., Poeck, H., Akira, S., Conzelmann, K.K., Schlee, M.*, et al.* (2006). 5'-Triphosphate RNA is the ligand for RIG-I. Science *314*, 994-997.

Hou, F., Sun, L., Zheng, H., Skaug, B., Jiang, Q.X., and Chen, Z.J. (2011). MAVS forms functional prion-like aggregates to activate and propagate antiviral innate immune response. Cell *146*, 448-461.

Iwamoto, F., Stadler, M., Chalupnikova, K., Oakeley, E., and Nagamine, Y. (2008). Transcription-dependent nucleolar cap localization and possible

nuclear function of DExH RNA helicase RHAU. Experimental cell research *314*, 1378-1391.

Iwamura, T., Yoneyama, M., Yamaguchi, K., Suhara, W., Mori, W., Shiota, K., Okabe, Y., Namiki, H., and Fujita, T. (2001). Induction of IRF-3/-7 kinase and NF-kappaB in response to double-stranded RNA and virus infection: common and unique pathways. Genes to cells : devoted to molecular & cellular mechanisms *6*, 375-388.

Jiang, F., Ramanathan, A., Miller, M.T., Tang, G.Q., Gale, M., Jr., Patel, S.S., and Marcotrigiano, J. (2011). Structural basis of RNA recognition and activation by innate immune receptor RIG-I. Nature *479*, 423-427.

Jiang, X., Kinch, L.N., Brautigam, C.A., Chen, X., Du, F., Grishin, N.V., and Chen, Z.J. (2012). Ubiquitin-induced oligomerization of the RNA sensors RIG-I and MDA5 activates antiviral innate immune response. Immunity *36*, 959-973.

Kageyama, M., Takahasi, K., Narita, R., Hirai, R., Yoneyama, M., Kato, H., and Fujita, T. (2011). 55 Amino acid linker between helicase and carboxyl terminal domains of RIG-I functions as a critical repression domain and determines inter-domain conformation. Biochemical and biophysical research communications *415*, 75-81.

Kato, H., Sato, S., Yoneyama, M., Yamamoto, M., Uematsu, S., Matsui, K., Tsujimura, T., Takeda, K., Fujita, T., Takeuchi, O.*, et al.* (2005). Cell type-specific involvement of RIG-I in antiviral response. Immunity *23*, 19-28.

Kato, H., Takahasi, K., and Fujita, T. (2011). RIG-I-like receptors: cytoplasmic sensors for non-self RNA. Immunological reviews *243*, 91-98.

Kato, H., Takeuchi, O., Mikamo-Satoh, E., Hirai, R., Kawai, T., Matsushita, K., Hiiragi, A., Dermody, T.S., Fujita, T., and Akira, S. (2008). Length-dependent recognition of double-stranded ribonucleic acids by retinoic acid-inducible gene-I and melanoma differentiation-associated gene 5. The Journal of experimental medicine *205*, 1601-1610.

Kato, H., Takeuchi, O., Sato, S., Yoneyama, M., Yamamoto, M., Matsui, K., Uematsu, S., Jung, A., Kawai, T., Ishii, K.J.*, et al.* (2006). Differential roles of MDA5 and RIG-I helicases in the recognition of RNA viruses. Nature *441*, 101-105.

Kawai, T., and Akira, S. (2009). The roles of TLRs, RLRs and NLRs in pathogen recognition. Int Immunol *21*, 317-337.

Kawai, T., and Akira, S. (2011). Toll-like receptors and their crosstalk with other innate receptors in infection and immunity. Immunity *34*, 637-650.

Kawai, T., Takahashi, K., Sato, S., Coban, C., Kumar, H., Kato, H., Ishii, K.J., Takeuchi, O., and Akira, S. (2005). IPS-1, an adaptor triggering RIG-I- and Mda5-mediated type I interferon induction. Nature immunology *6*, 981-988.

Kim, T., Pazhoor, S., Bao, M., Zhang, Z., Hanabuchi, S., Facchinetti, V., Bover, L., Plumas, J., Chaperot, L., Qin, J.*, et al.* (2010). Aspartate-glutamate-alanine-histidine box motif (DEAH)/RNA helicase A helicases sense microbial DNA in human plasmacytoid dendritic cells. Proceedings of the National Academy of Sciences of the United States of America *107*, 15181-15186.

Kowalinski, E., Lunardi, T., McCarthy, A.A., Louber, J., Brunel, J., Grigorov, B., Gerlier, D., and Cusack, S. (2011). Structural basis for the activation of innate immune pattern-recognition receptor RIG-I by viral RNA. Cell *147*, 423-435.

Kumar, H., Kawai, T., Kato, H., Sato, S., Takahashi, K., Coban, C., Yamamoto, M., Uematsu, S., Ishii, K.J., Takeuchi, O.*, et al.* (2006). Essential role of IPS-1 in innate immune responses against RNA viruses. The Journal of experimental medicine *203*, 1795-1803.

Lai, J.C., Ponti, S., Pan, D., Kohler, H., Skoda, R.C., Matthias, P., and Nagamine, Y. (2012). The DEAH-box helicase RHAU is an essential gene and critical for mouse hematopoiesis. Blood *119*, 4291-4300.

Lattmann, S., Giri, B., Vaughn, J.P., Akman, S.A., and Nagamine, Y. (2010). Role of the amino terminal RHAU-specific motif in the recognition and resolution of guanine quadruplex-RNA by the DEAH-box RNA helicase RHAU. Nucleic acids research *38*, 6219-6233.

Lu, B., Nakamura, T., Inouye, K., Li, J., Tang, Y., Lundback, P., Valdes-Ferrer, S.I., Olofsson, P.S., Kalb, T., Roth, J.*, et al.* (2012). Novel role of PKR in inflammasome activation and HMGB1 release. Nature *488*, 670-674.

Lu, J., O'Hara, E.B., Trieselmann, B.A., Romano, P.R., and Dever, T.E. (1999). The interferon-induced double-stranded RNA-activated protein kinase PKR will phosphorylate serine, threonine, or tyrosine at residue 51 in eukaryotic initiation factor 2alpha. The Journal of biological chemistry *274*, 32198-32203.

Luthra, P., Sun, D., Silverman, R.H., and He, B. (2011). Activation of IFN-β expression by a viral mRNA through RNase L and MDA5. Proceedings of the National Academy of Sciences of the United States of America *108*, 2118-2123.

Malathi, K., Dong, B., Gale, M., Jr., and Silverman, R.H. (2007). Small self-RNA generated by RNase L amplifies antiviral innate immunity. Nature *448*, 816-819.

Malathi, K., Saito, T., Crochet, N., Barton, D.J., Gale, M., Jr., and Silverman, R.H. (2010). RNase L releases a small RNA from HCV RNA that refolds into a potent PAMP. RNA *16*, 2108-2119.

Matsui, T., Tanihara, K., and Date, T. (2001). Expression of unphosphorylated form of human double-stranded RNA-activated protein kinase in Escherichia coli. Biochemical and biophysical research communications *284*, 798-807.

McAllister, C.S., Toth, A.M., Zhang, P., Devaux, P., Cattaneo, R., and Samuel, C.E. (2010). Mechanisms of protein kinase PKR-mediated amplification of beta interferon induction by C protein-deficient measles virus. Journal of virology *84*, 380-386.

Meylan, E., Curran, J., Hofmann, K., Moradpour, D., Binder, M., Bartenschlager, R., and Tschopp, J. (2005). Cardif is an adaptor protein in the RIG-I antiviral pathway and is targeted by hepatitis C virus. Nature *437*, 1167-1172.

Momose, F., Kikuchi, Y., Komase, K., and Morikawa, Y. (2007). Visualization of microtubule-mediated transport of influenza viral progeny ribonucleoprotein. Microbes and infection / Institut Pasteur *9*, 1422-1433.

Nallagatla, S.R., Hwang, J., Toroney, R., Zheng, X., Cameron, C.E., and Bevilacqua, P.C. (2007). 5'-triphosphate-dependent activation of PKR by RNAs with short stem-loops. Science *318*, 1455-1458.

Ng, C.S., Jogi, M., Yoo, J.S., Onomoto, K., Koike, S., Iwasaki, T., Yoneyama, M., Kato, H., and Fujita, T. (2013). Encephalomyocarditis virus disrupts stress granules, the critical platform for triggering antiviral innate immune responses. Journal of virology *87*, 9511-9522.

Ng, C.S., Kato, H., and Fujita, T. (2012). Recognition of viruses in the cytoplasm by RLRs and other helicases--how conformational changes, mitochondrial dynamics and ubiquitination control innate immune responses. Int Immunol *24*, 739-749.

Okonski, K.M., and Samuel, C.E. (2013). Stress granule formation induced by measles virus is protein kinase PKR dependent and impaired by RNA adenosine deaminase ADAR1. Journal of virology *87*, 756-766.

Onoguchi, K., Onomoto, K., Takamatsu, S., Jogi, M., Takemura, A., Morimoto, S., Julkunen, I., Namiki, H., Yoneyama, M., and Fujita, T. (2010). Virus-infection or 5'ppp-RNA activates antiviral signal through redistribution of IPS-1 mediated by MFN1. PLoS pathogens *6*, e1001012.

Onomoto, K., Jogi, M., Yoo, J.S., Narita, R., Morimoto, S., Takemura, A., Sambhara, S., Kawaguchi, A., Osari, S., Nagata, K.*, et al.* (2012). Critical role of an antiviral stress granule containing RIG-I and PKR in viral detection and innate immunity. PloS one *7*, e43031.

Panda, D., Dinh, P.X., Beura, L.K., and Pattnaik, A.K. (2010). Induction of interferon and interferon signaling pathways by replication of defective interfering particle RNA in cells constitutively expressing vesicular stomatitis virus replication proteins. Journal of virology *84*, 4826-4831.

Patel, J.R., Jain, A., Chou, Y.Y., Baum, A., Ha, T., and Garcia-Sastre, A. (2013). ATPase-driven oligomerization of RIG-I on RNA allows optimal activation of type-I interferon. EMBO reports *14*, 780-787.

Peisley, A., Wu, B., Xu, H., Chen, Z.J., and Hur, S. (2014). Structural basis for ubiquitin-mediated antiviral signal activation by RIG-I. Nature.

Pichlmair, A., Schulz, O., Tan, C.P., Naslund, T.I., Liljestrom, P., Weber, F., and Reis e Sousa, C. (2006). RIG-I-mediated antiviral responses to single-stranded RNA bearing 5'-phosphates. Science *314*, 997-1001.

Pichlmair, A., Schulz, O., Tan, C.P., Rehwinkel, J., Kato, H., Takeuchi, O., Akira, S., Way, M., Schiavo, G., and Reis e Sousa, C. (2009). Activation of MDA5 requires higher-order RNA structures generated during virus infection. Journal of virology *83*, 10761-10769.

Pindel, A., and Sadler, A. (2011). The role of protein kinase R in the interferon response. Journal of interferon & cytokine research : the official journal of the International Society for Interferon and Cytokine Research *31*, 59-70.

Rajsbaum, R., Garcia-Sastre, A., and Versteeg, G.A. (2014). TRIMmunity: The Roles of the TRIM E3-Ubiquitin Ligase Family in Innate Antiviral Immunity. Journal of molecular biology *426*, 1265-1284.

Rehwinkel, J., Tan, C.P., Goubau, D., Schulz, O., Pichlmair, A., Bier, K., Robb, N., Vreede, F., Barclay, W., Fodor, E.*, et al.* (2010). RIG-I detects viral genomic RNA during negative-strand RNA virus infection. Cell *140*, 397-408.

Saito, T., Owen, D.M., Jiang, F., Marcotrigiano, J., and Gale, M., Jr. (2008). Innate immunity induced by composition-dependent RIG-I recognition of hepatitis C virus RNA. Nature *454*, 523-527.

Satoh, T., Kato, H., Kumagai, Y., Yoneyama, M., Sato, S., Matsushita, K., Tsujimura, T., Fujita, T., Akira, S., and Takeuchi, O. (2010). LGP2 is a positive regulator of RIG-I- and MDA5-mediated antiviral responses. Proceedings of the National Academy of Sciences of the United States of America *107*, 1512-1517.

Schlee, M., Roth, A., Hornung, V., Hagmann, C.A., Wimmenauer, V., Barchet, W., Coch, C., Janke, M., Mihailovic, A., Wardle, G.*, et al.* (2009). Recognition of 5' triphosphate by RIG-I helicase requires short blunt double-stranded RNA as contained in panhandle of negative-strand virus. Immunity *31*, 25-34.

Schmidt, A., Schwerd, T., Hamm, W., Hellmuth, J.C., Cui, S., Wenzel, M., Hoffmann, F.S., Michallet, M.C., Besch, R., Hopfner, K.P.*, et al.* (2009). 5'-triphosphate RNA requires base-paired structures to activate antiviral signaling via RIG-I. Proceedings of the National Academy of Sciences of the United States of America *106*, 12067-12072.

Schulz, O., Pichlmair, A., Rehwinkel, J., Rogers, N.C., Scheuner, D., Kato, H., Takeuchi, O., Akira, S., Kaufman, R.J., and Reis e Sousa, C. (2010). Protein kinase R contributes to immunity against specific viruses by regulating interferon mRNA integrity. Cell host & microbe *7*, 354-361.

Sen, A., Pruijssers, A.J., Dermody, T.S., Garcia-Sastre, A., and Greenberg, H.B. (2011). The early interferon response to rotavirus is regulated by PKR and depends on MAVS/IPS-1, RIG-I, MDA-5, and IRF3. Journal of virology *85*, 3717-3732.

Seth, R.B., Sun, L., Ea, C.K., and Chen, Z.J. (2005). Identification and characterization of MAVS, a mitochondrial antiviral signaling protein that activates NF-kappaB and IRF 3. Cell *122*, 669-682.

Simpson-Holley, M., Kedersha, N., Dower, K., Rubins, K.H., Anderson, P., Hensley, L.E., and Connor, J.H. (2011). Formation of antiviral cytoplasmic granules during orthopoxvirus infection. Journal of virology *85*, 1581-1593.

Sun, Q., Sun, L., Liu, H.H., Chen, X., Seth, R.B., Forman, J., and Chen, Z.J. (2006). The specific and essential role of MAVS in antiviral innate immune responses. Immunity *24*, 633-642.

Takahasi, K., Yoneyama, M., Nishihori, T., Hirai, R., Kumeta, H., Narita, R., Gale, M., Jr., Inagaki, F., and Fujita, T. (2008). Nonself RNA-sensing mechanism of RIG-I helicase and activation of antiviral immune responses. Molecular cell *29*, 428-440.

Tran, H., Schilling, M., Wirbelauer, C., Hess, D., and Nagamine, Y. (2004). Facilitation of mRNA deadenylation and decay by the exosome-bound, DExH protein RHAU. Molecular cell *13*, 101-111.

Valiente-Echeverria, F., Melnychuk, L., and Mouland, A.J. (2012). Viral modulation of stress granules. Virus research *169*, 430-437.

Wang, Y., Ludwig, J., Schuberth, C., Goldeck, M., Schlee, M., Li, H., Juranek, S., Sheng, G., Micura, R., Tuschl, T.*, et al.* (2010). Structural and functional insights into 5'-ppp RNA pattern recognition by the innate immune receptor RIG-I. Nature structural & molecular biology *17*, 781-787.

White, J.P., and Lloyd, R.E. (2012). Regulation of stress granules in virus systems. Trends in microbiology *20*, 175-183.

Witteveldt, J., Blundell, R., Maarleveld, J.J., McFadden, N., Evans, D.J., and Simmonds, P. (2014). The influence of viral RNA secondary structure on interactions with innate host cell defences. Nucleic acids research *42*, 3314-3329.

Xu, L.G., Wang, Y.Y., Han, K.J., Li, L.Y., Zhai, Z., and Shu, H.B. (2005). VISA is an adapter protein required for virus-triggered IFN-beta signaling. Molecular cell *19*, 727-740.

Yoneyama, M., and Fujita, T. (2007). Function of RIG-I-like receptors in antiviral innate immunity. The Journal of biological chemistry *282*, 15315-15318.

Yoneyama, M., Kikuchi, M., Matsumoto, K., Imaizumi, T., Miyagishi, M., Taira, K., Foy, E., Loo, Y.M., Gale, M., Jr., Akira, S.*, et al.* (2005). Shared and unique functions of the DExD/H-box helicases RIG-I, MDA5, and LGP2 in antiviral innate immunity. Journal of immunology *175*, 2851-2858.

Yoneyama, M., Kikuchi, M., Natsukawa, T., Shinobu, N., Imaizumi, T., Miyagishi, M., Taira, K., Akira, S., and Fujita, T. (2004). The RNA helicase RIG-I has an essential function in double-stranded RNA-induced innate antiviral responses. Nature immunology *5*, 730-737.

Zhang, Z., Kim, T., Bao, M., Facchinetti, V., Jung, S.Y., Ghaffari, A.A., Qin, J., Cheng, G., and Liu, Y.J. (2011). DDX1, DDX21, and DHX36 helicases form a complex with the adaptor molecule TRIF to sense dsRNA in dendritic cells. Immunity *34*, 866-878.

Tables

1. RLR agonists

1-1 List of RNA ligands

	RNAs / Viruses	Characteristics	Sensor	References
Artificial RNA	5' ppp copy-back RNA	In vitro transcribed RNA	RIG-I	Schlee (2009), Schmidt (2009)
	5'ppp AU-rich RNA	Pol III product from poly dA:dT	RIG-I	Ablasser (2009), Chiu (2009)
	poly I:C short	Short dsRNA (< 1 kb)	RIG-I	Kato (2008)
	poly I:C long	Long dsRNA (> 7 kb)	MDA5	Kato (2008)
Natural RNA	IAV genomic RNA	5' ppp with panhandle structure	RIG-I	Rehwinkel (2010)
	HCV 3'UTR U/UC rich RNA	5' ppp dependent	RIG-I	Saito (2008)
	IAV 3'UTR U/A rich RNA	5' ppp independent	RIG-I	Davis (2012)
	SeV, VSV DI RNA	5' ppp copy-back dsRNA	RIG-I	Strahle (2006), Patel (2013), Panda (2010)
	VV, EMCV	High molecular weight RNA	MDA5	Pichlmair (2009)
	CVB3, Mengo	Replication intermediates	MDA5	Feng (2012)
	PIV5 L mRNA	RNase L product	MDA5	Luthra (2011)
	EMCV L antisense	LGP2-interacting RNA	MDA5 / LGP2	Deddouche (2014)
Host RNA	5'OH-3'p short RNA	RNase L product	RIG-I / MDA5	Malathi (2007)

1-2 List of viruses and their known sensors

Sensor	Viruses	Families / Genome	References
RIG-I	Newcastle disease virus	Paramyxoviridae / (−) ssRNA, non-segmented	Kato (2006)
	Sendai virus		Yoneyama (2004), Kato (2006)
	Respiratory syncytical virus		Loo (2008)
	Vesicular stomatitis virus	Rhabdoviridae / (−) ssRNA, non-segmented	Yoneyama (2005), Kato (2006)
	Rabies virus		Hornung (2006)
	Influenza A virus	Orthomyxoviridae / (−) ssRNA, segmented	Kato (2006)
	Influenza B virus		Loo (2008)
	Rift Valley fever virus	Bunyaviridae / (−) ssRNA, segmented	Weber (2013)
	La Crosse virus		Weber (2013)
	Hepatitis C virus	Flaviviridae / (+) ssRNA, non-segmented	Saito (2008)
	Japanese encephalitis virus		Kato (2006)
	Epstein-Barr virus	Gammaherpesviridae / dsDNA	Samanta (2008)
MDA5	Encephalomyocarditis virus	Picornaviridae / (+) ssRNA, non-segmented	Kato (2006)
	Theiler's murine encephalitis virus		Kato (2006)
	Mengovirus		Kato (2006)
	Coxackie virus		Feng (2012)
	Entero virus		Feng (2012)
	Human Parechovirus		Feng (2012)
	Equine Rhinitis A virus		Feng (2012)
	Saffold virus		Feng (2012)
	Norovirus	Caliciviridae / (+) ssRNA, non-segmented	McCartney (2008)
	Vaccinia virus	Poxviridae / dsDNA	Pichlmair (2009)
RIG-I / MDA5	Westnile virus	Flaviviridae / (+) ssRNA, non-segmented	Loo (2008)
	Dengue viurs		Loo (2008)
	Measles virus	Paramyxoviridae / (−) ssRNA, non-segmented	Satoshi (2010)
	Semliki forest virus	Togaviridae / (+) ssRNA, non-segmented	Schulz (2010)

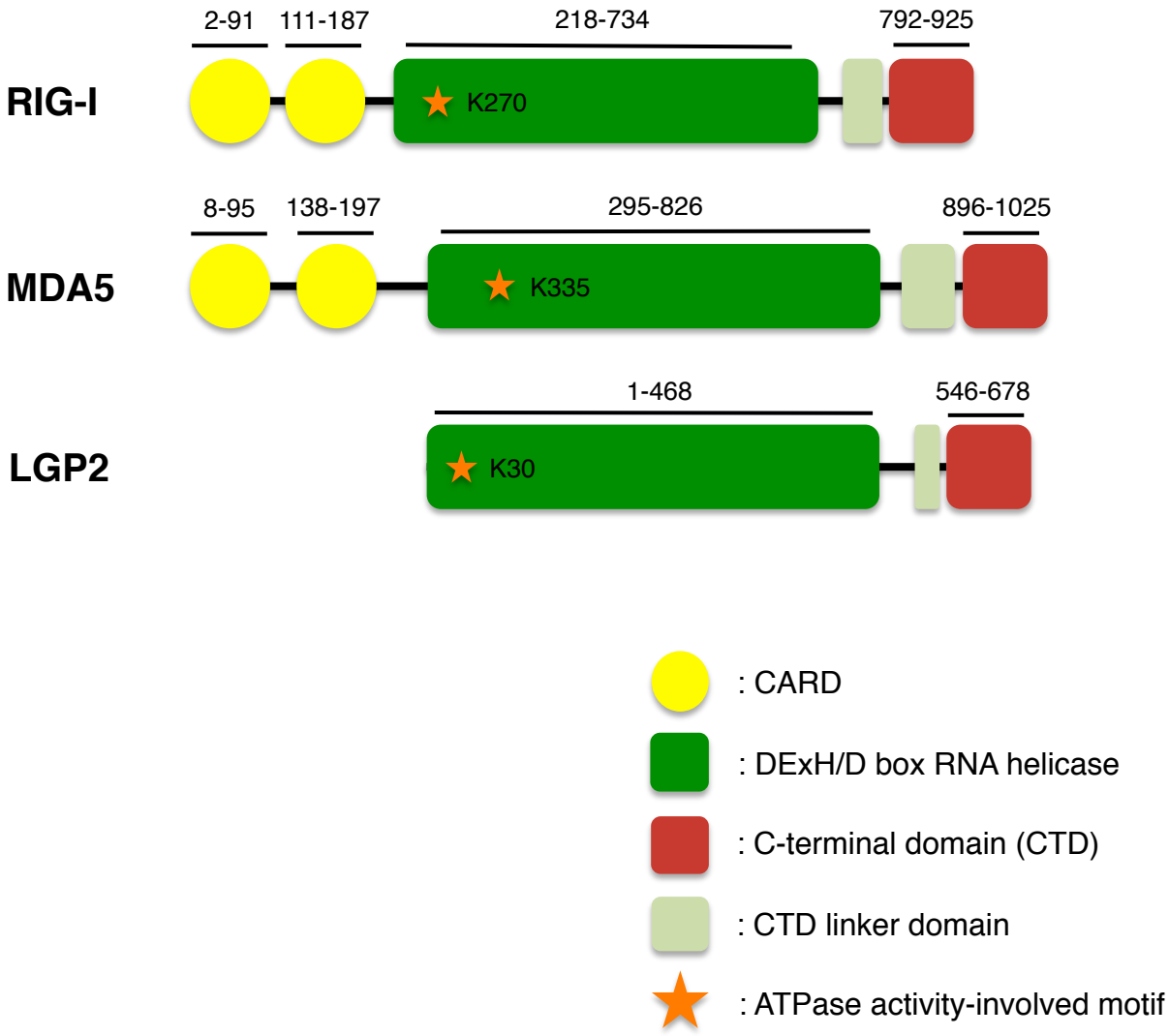

Fig 1. Schematic diagram of RLRs

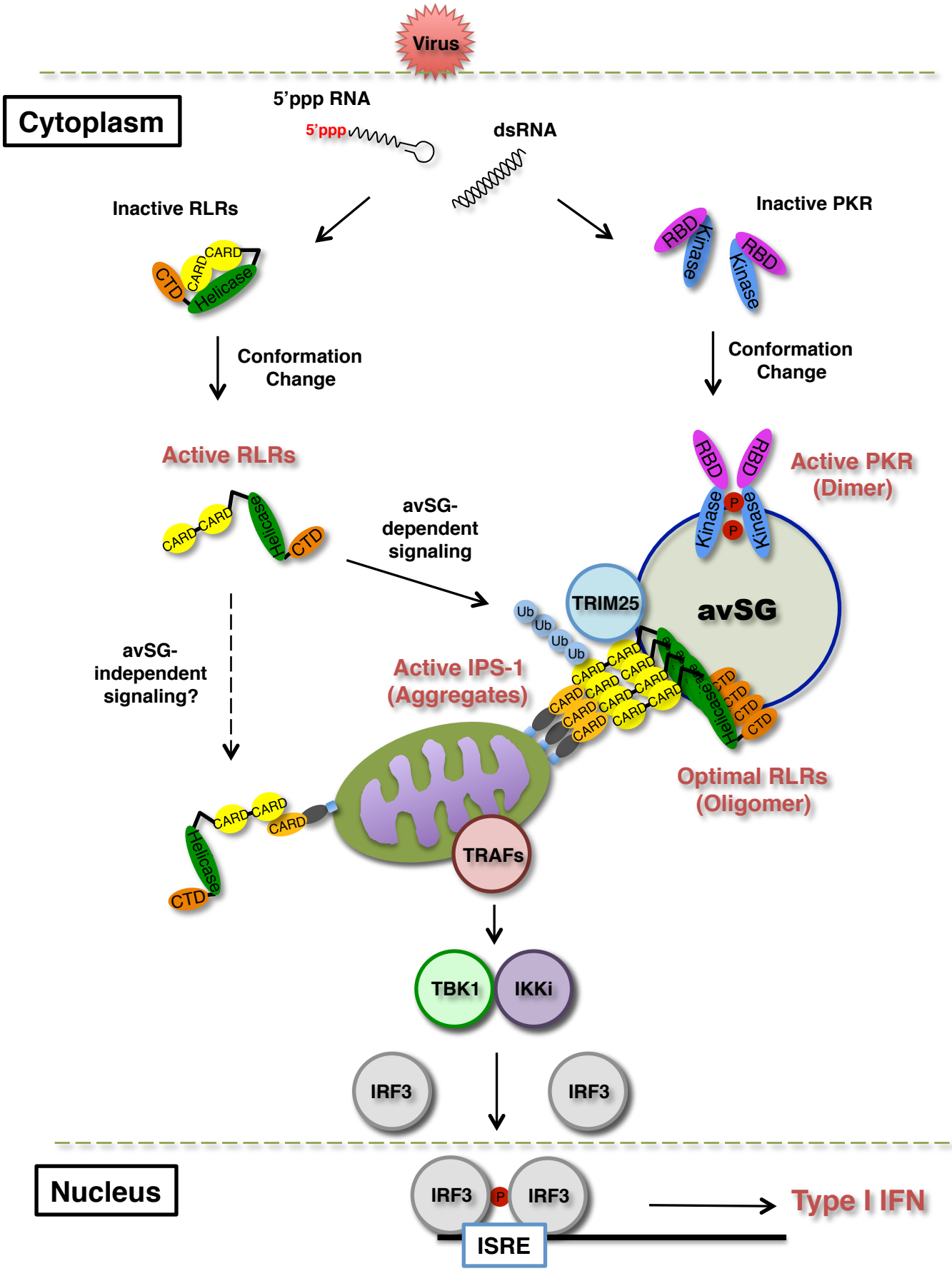

Fig 2. RLR signal pathway

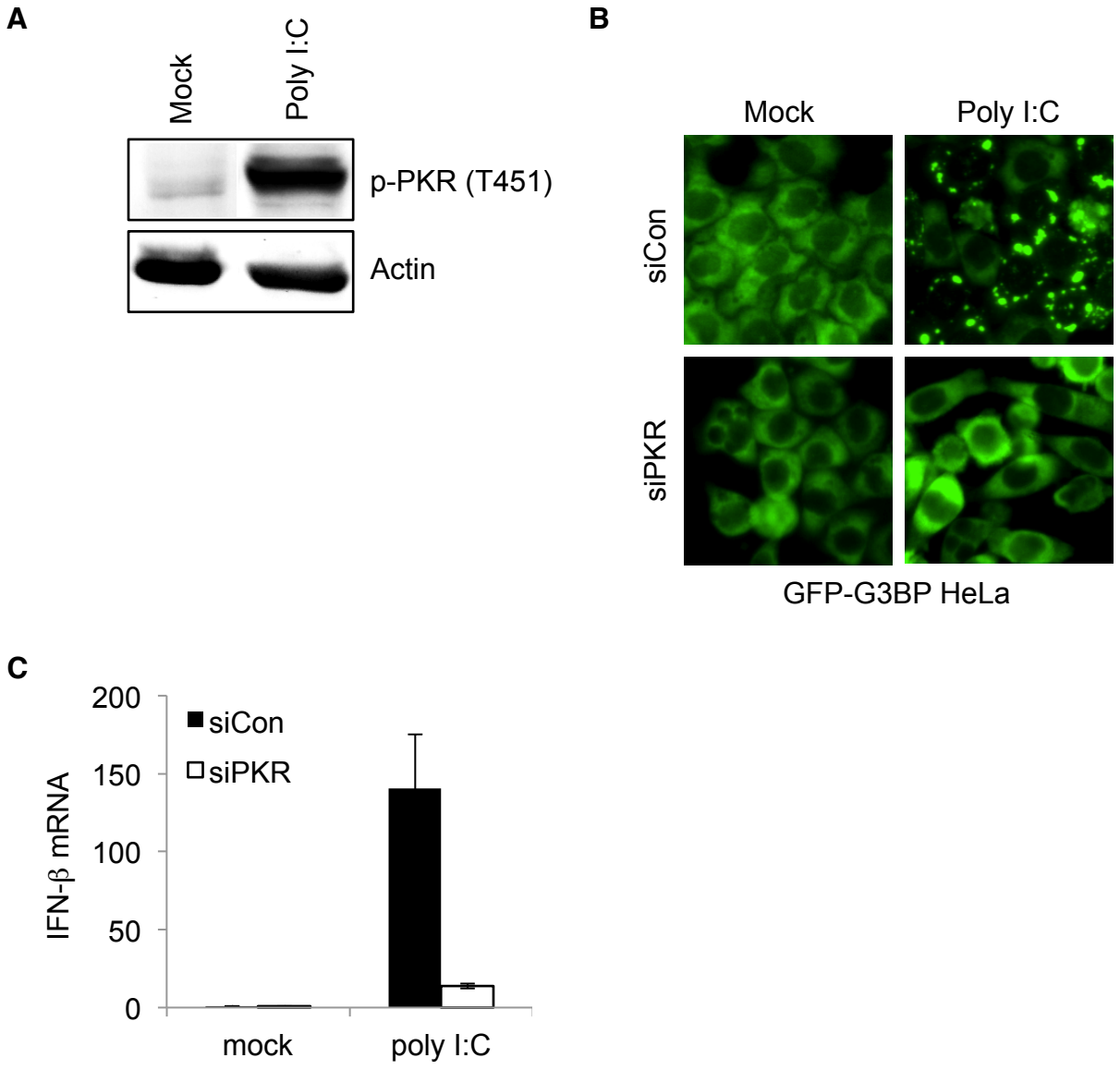

Fig 3. PKR regulates avSG formation and IFN signaling induced by dsRNA

A

- **5'ppp 27 nt:**
  5'- GGAAACUGAAAGGGAGAAGUGAAAGUG -3'

- **5'ppp 86 nt:**
  5'- GGGAUAUCAGCAAAGGAGAAGAACUUUUCACUGGAGUUGUCCCAAUUCUUGUUGAAUU
  AGGCCUCCCUUUAGUGAGGGUUAAUUGC -3'

- **5'ppp 136 nt:**
  5'- GGGAUAUCAGCAAAGGAGAAGAACUUUUCACUGGAGUUGUCCCAAUUCUUGUUGAAUU
  AGAUGGUGAUGUUAAUGGGCACAAAUUUUCUGUCAGUGGAGAGGGUGAAGAGGCCUCC
  CUUUAGUGAGGGUUAAUUGC -3'

B

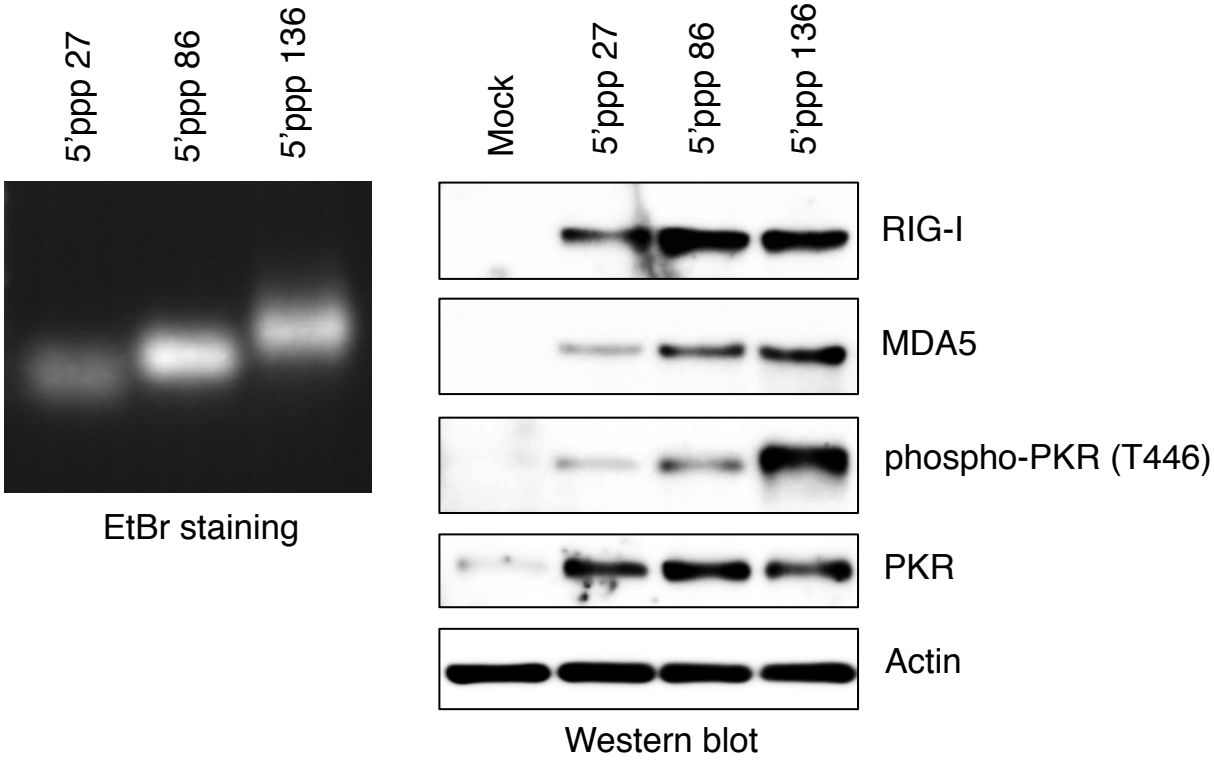

Fig 4. RNA length-dependent induction of antiviral protein expression

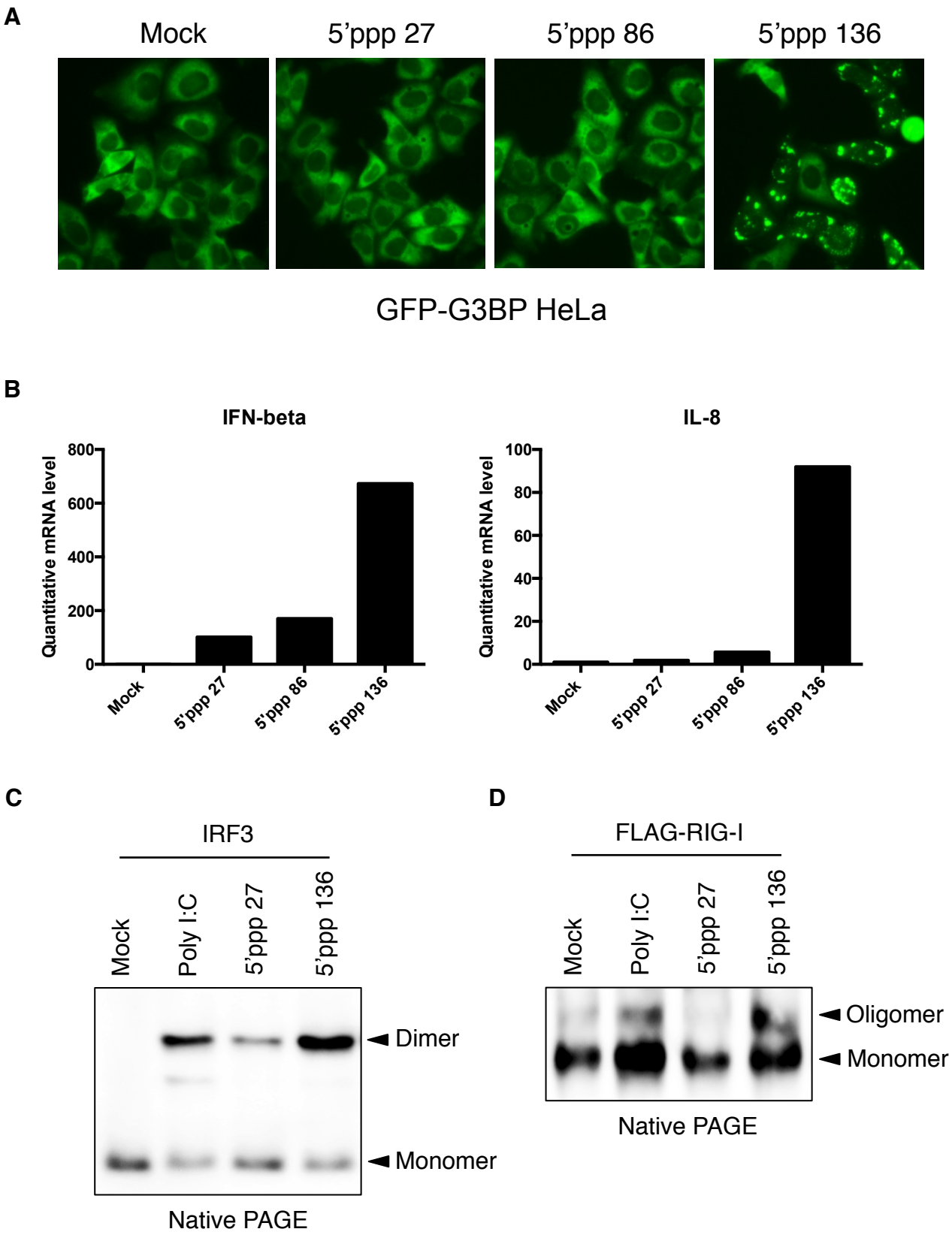

Fig 5. avSG enhances the expression of IFN and cytokine

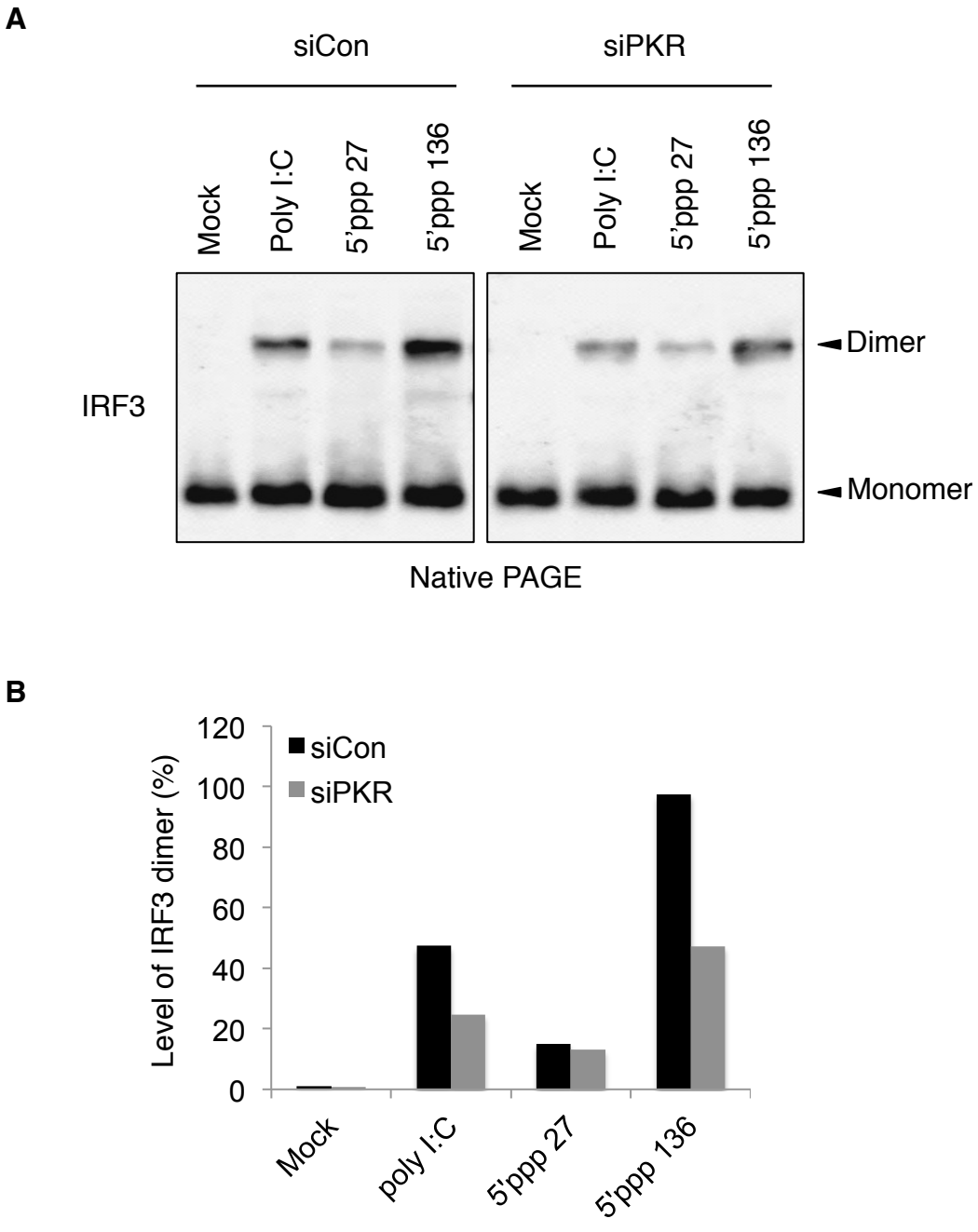

Fig 6. PKR regulates IFN signaling in a ligand-dependent manner

A

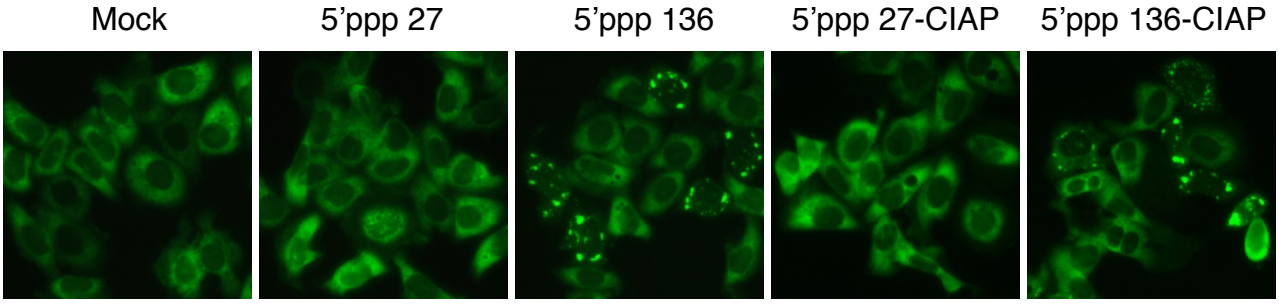

GFP-G3BP HeLa

B

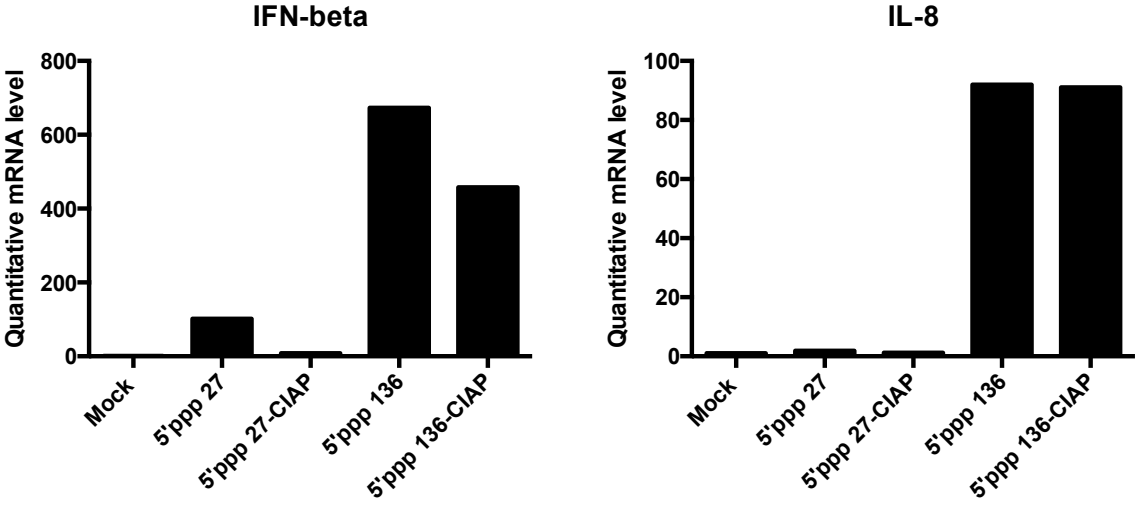

Fig 7. 5'ppp is not required for avSG-mediated antiviral signaling

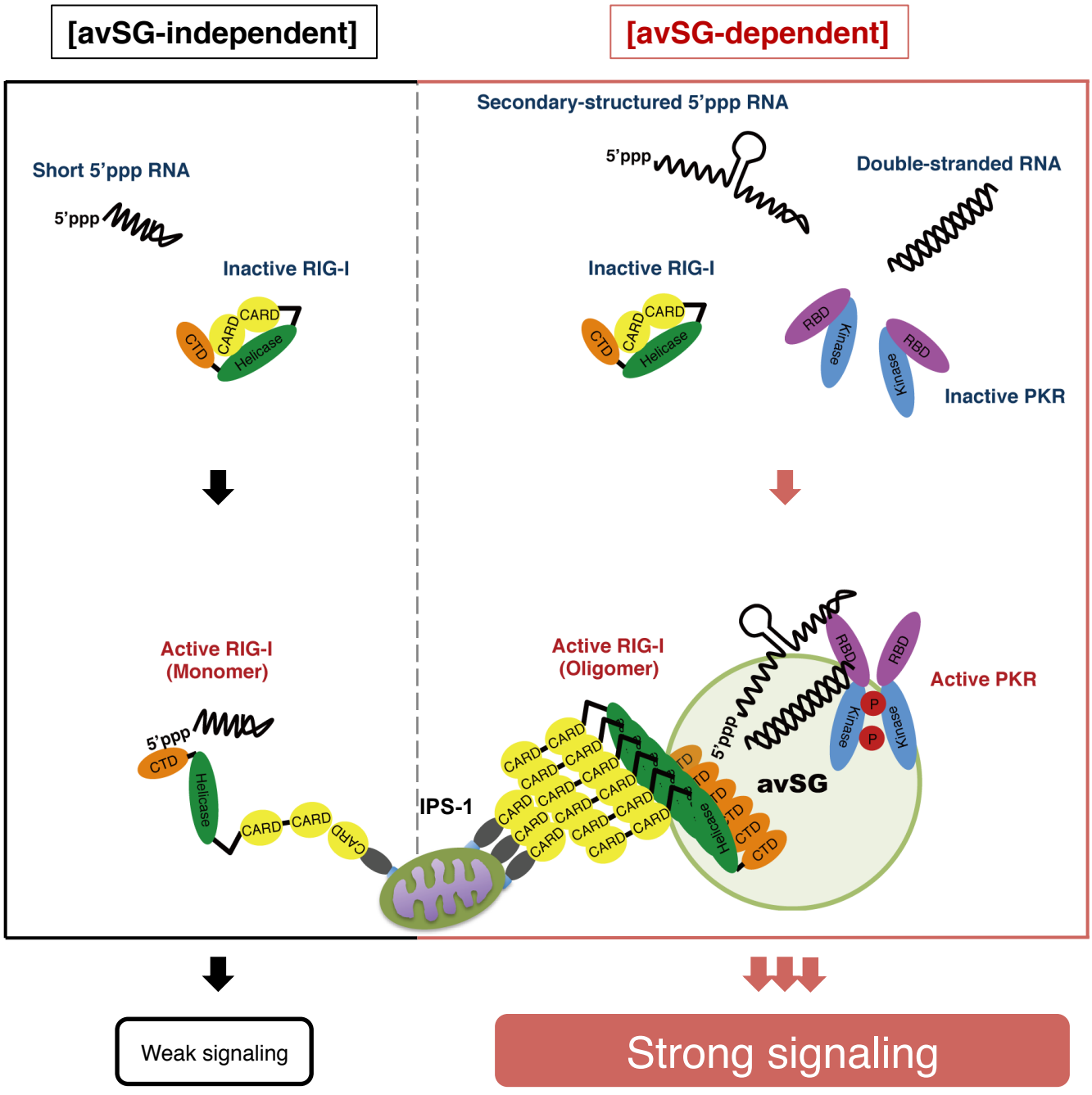

Fig 8. Hypothetical model

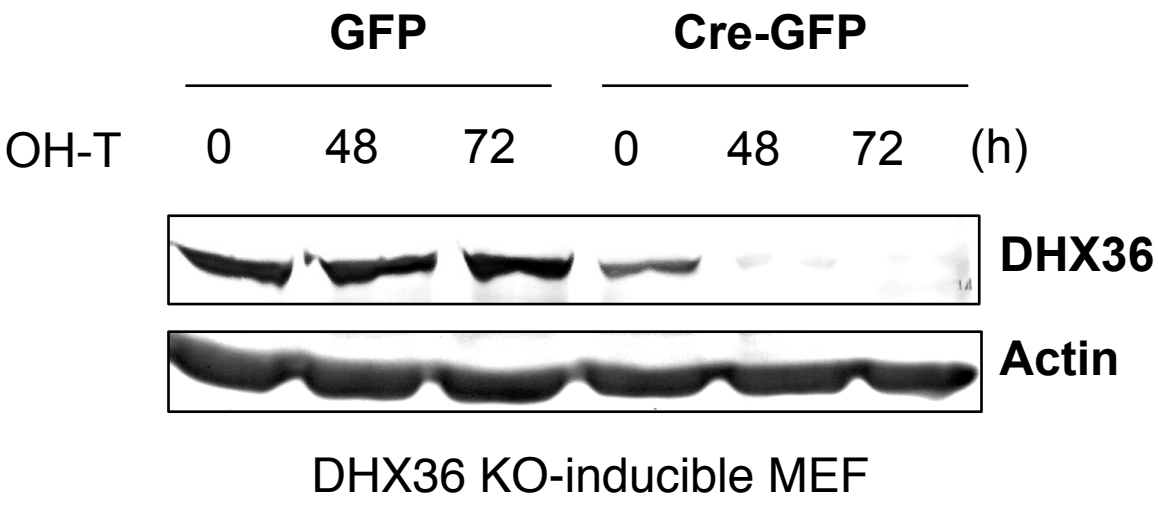

Fig 9. Confirmation of DHX36 level in DHX36 WT or KO-inducible MEF

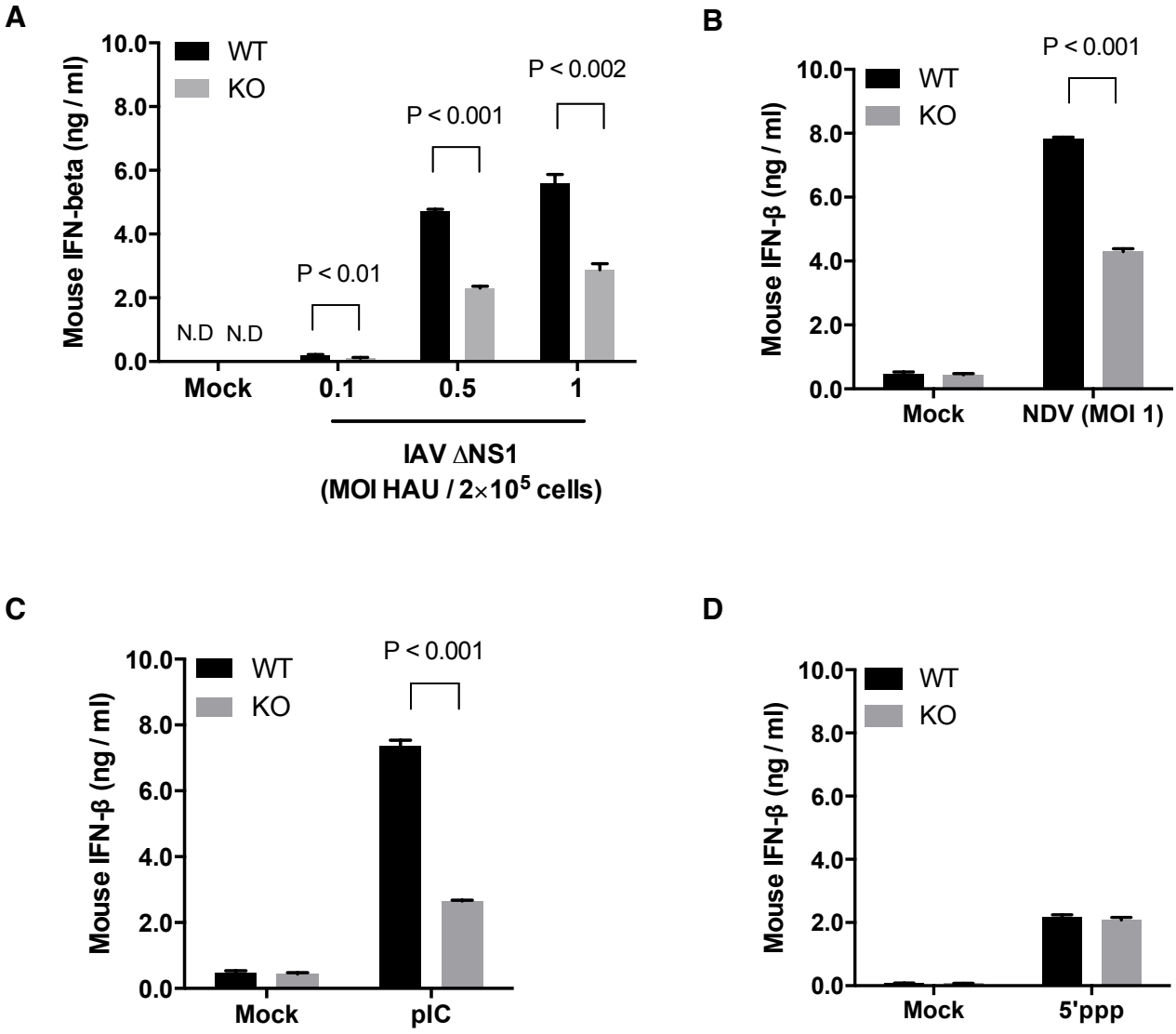

Fig 10. DHX36 regulates production of IFN-β in a stimulus-dependent manner

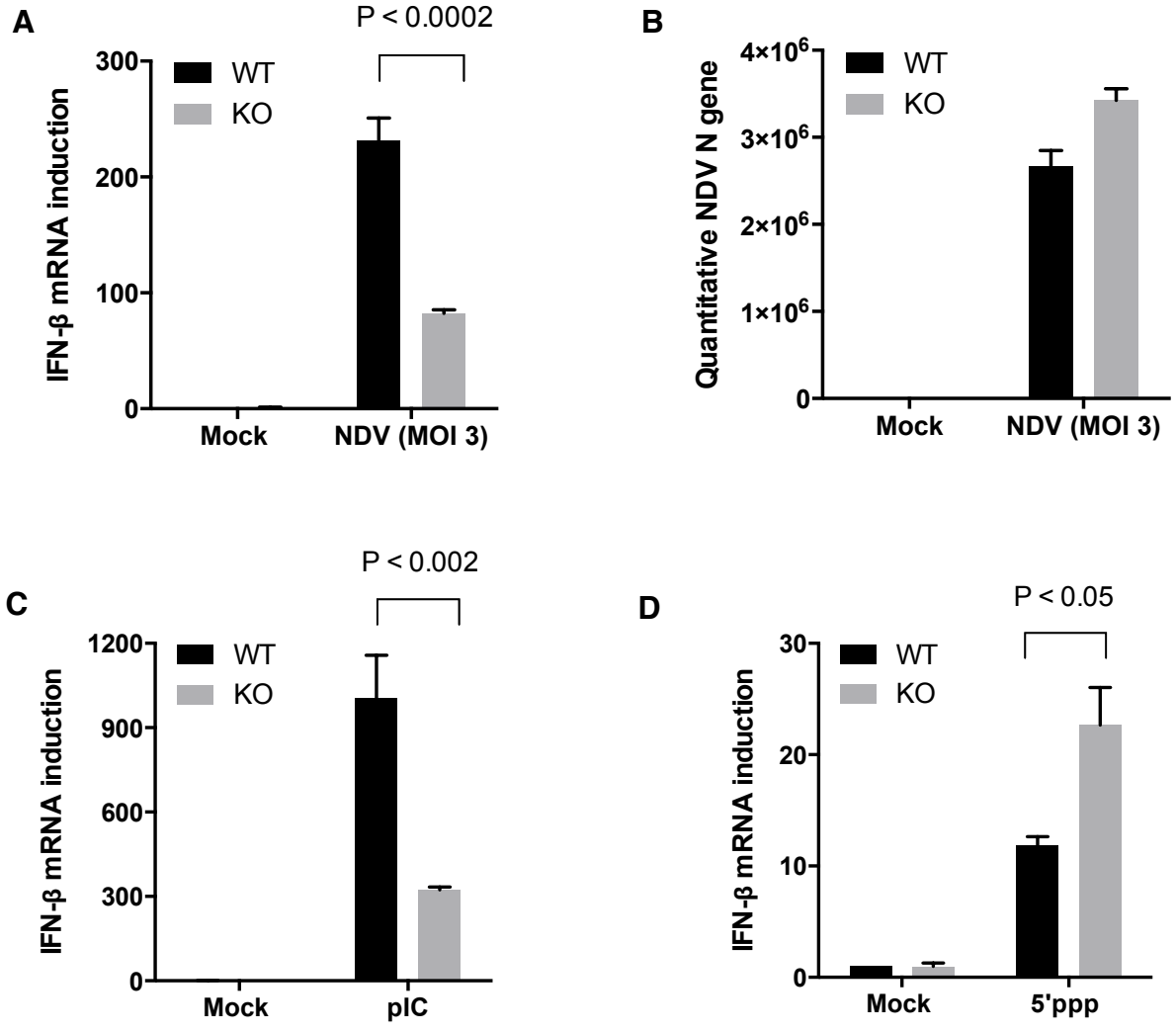

Fig 11. DHX36 regulates induction of IFN-β mRNA in a stimulus-dependent manner

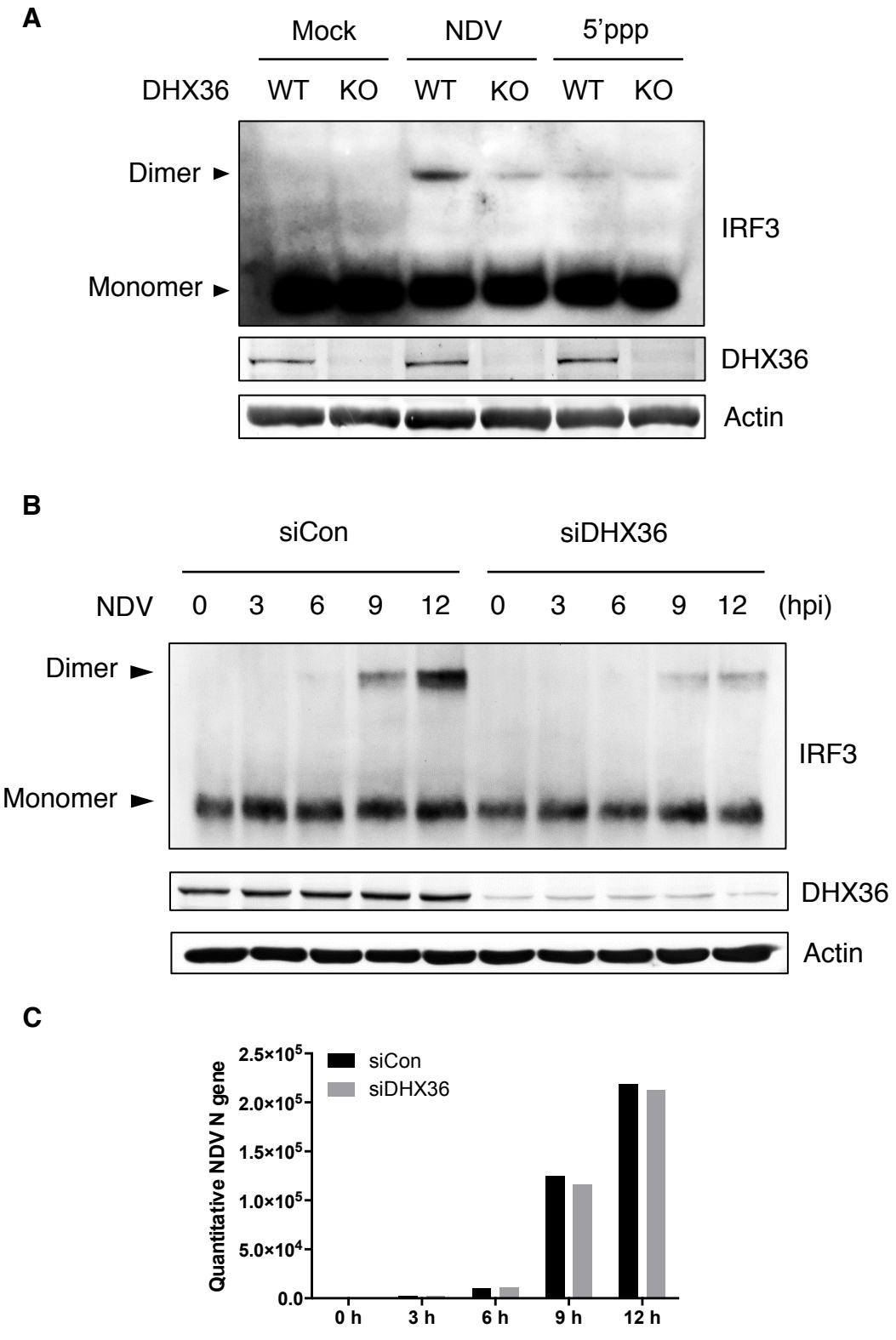

Fig 12. DHX36 regulates IFN signaling through IRF3 activation

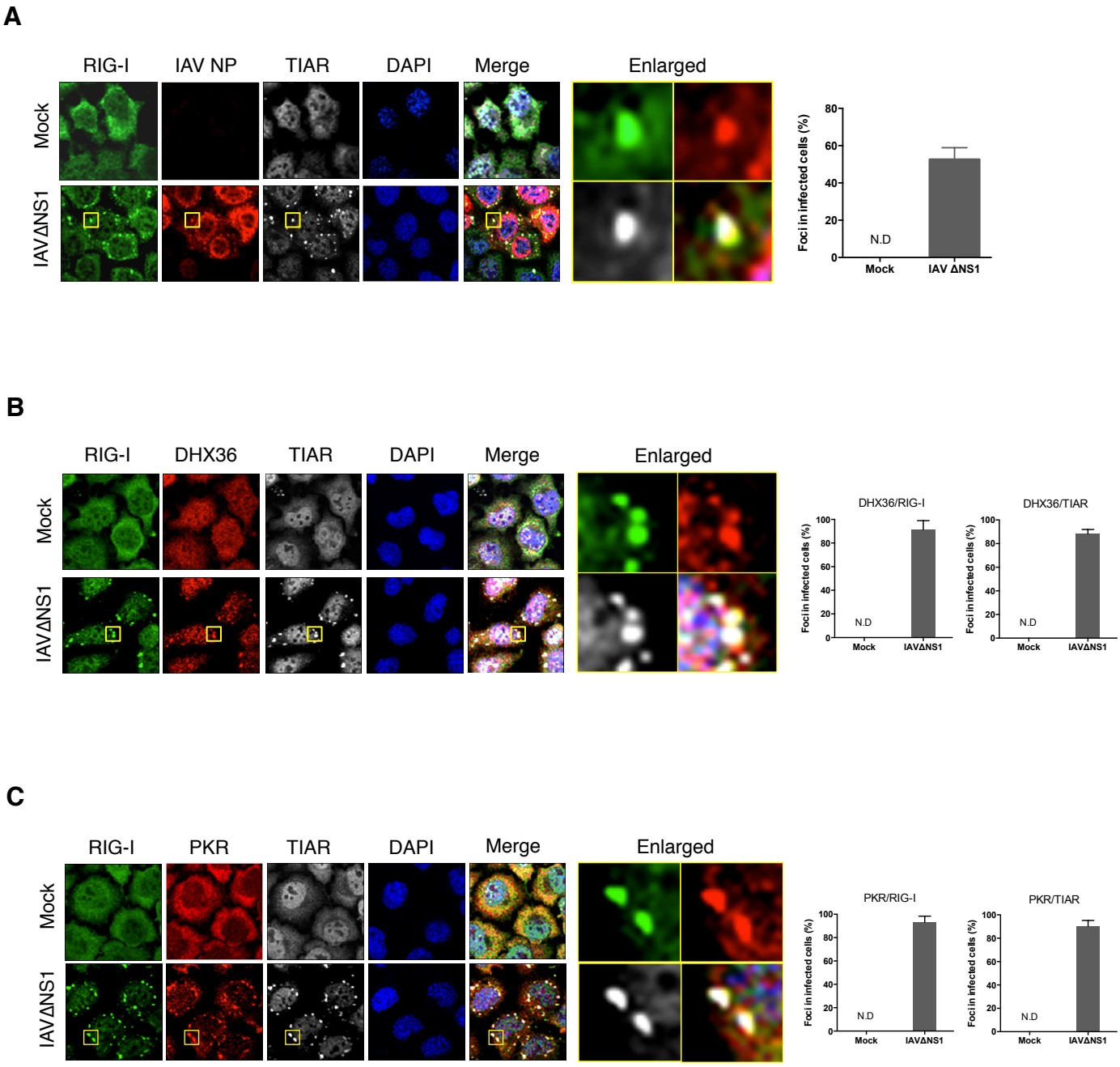

Fig 13. DHX36 localizes in the stress granules by virus infection

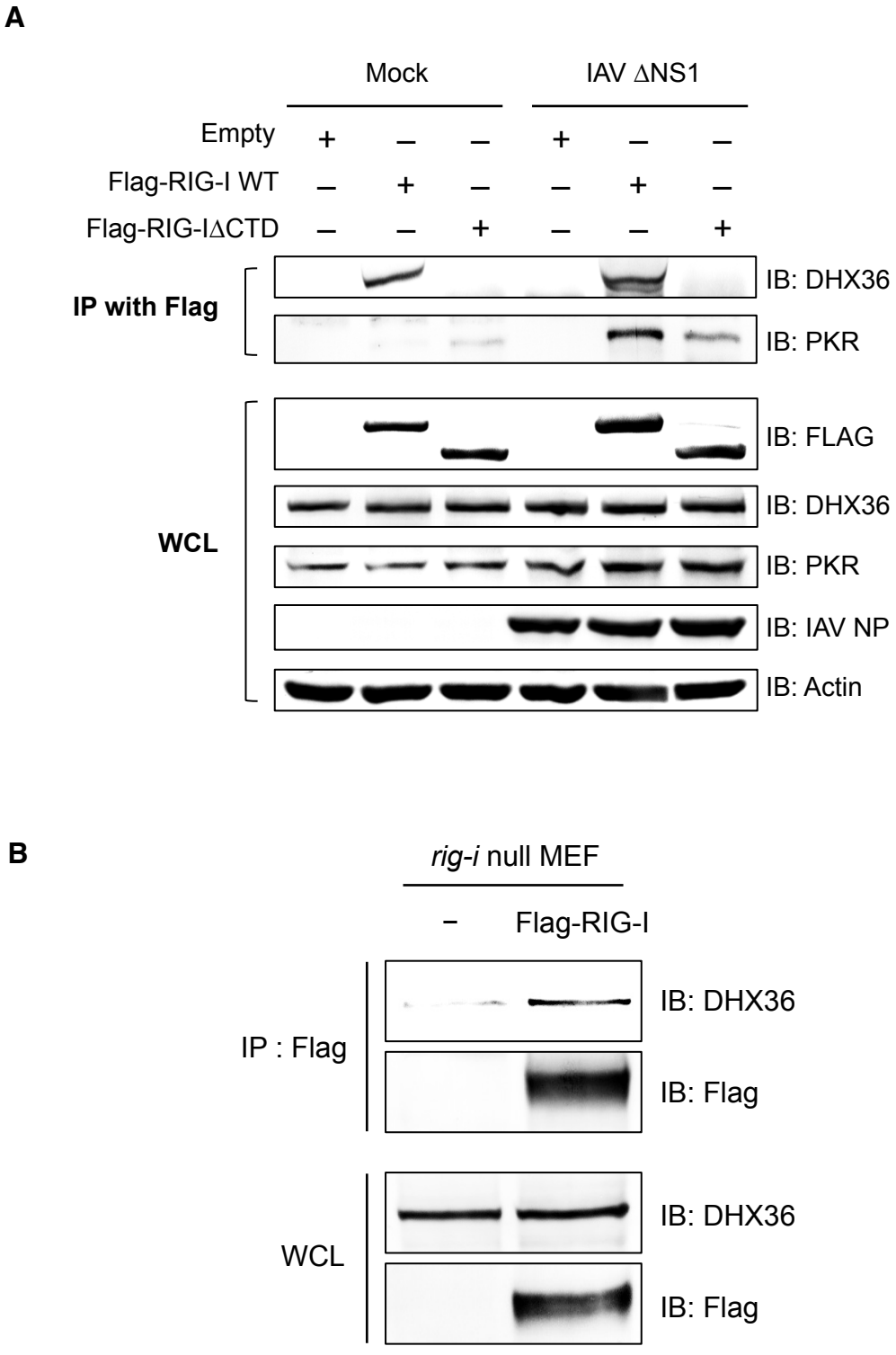

Fig 14. DHX36 interacts with antiviral proteins

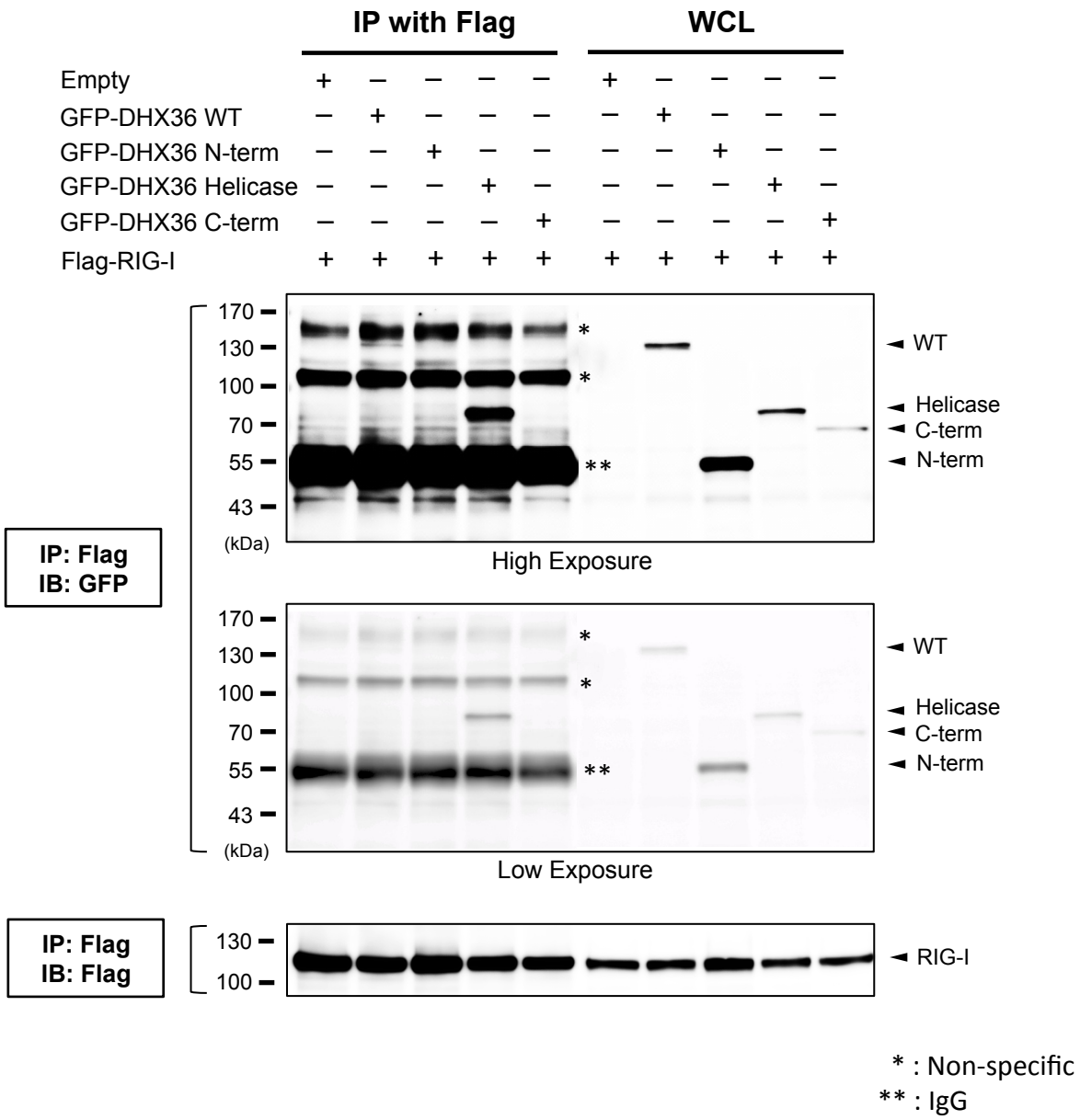

Fig 15. DHX36 interacts with RIG-I through its helicase domain

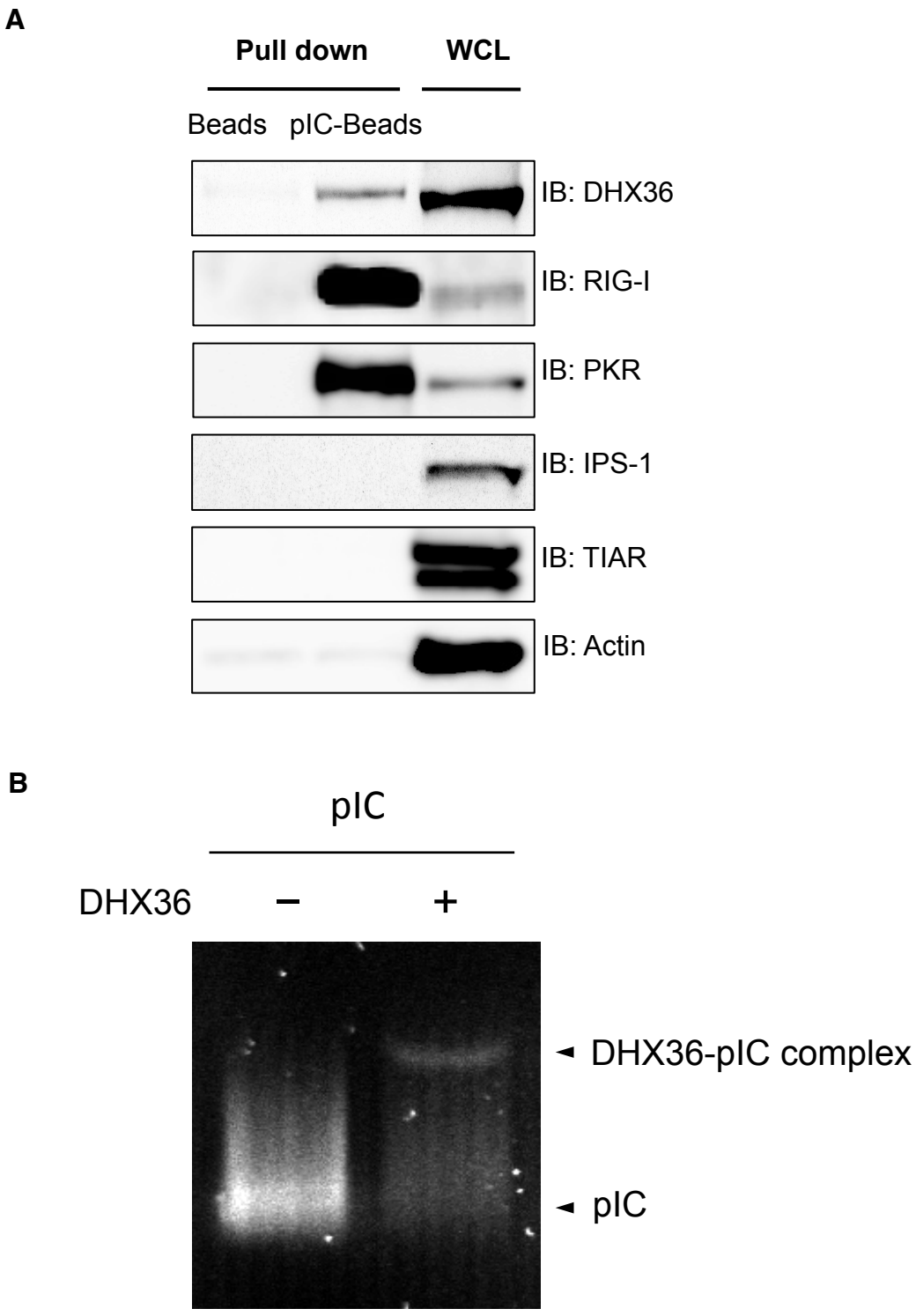

Fig 16. DHX36 forms a complex with antiviral proteins and dsRNA

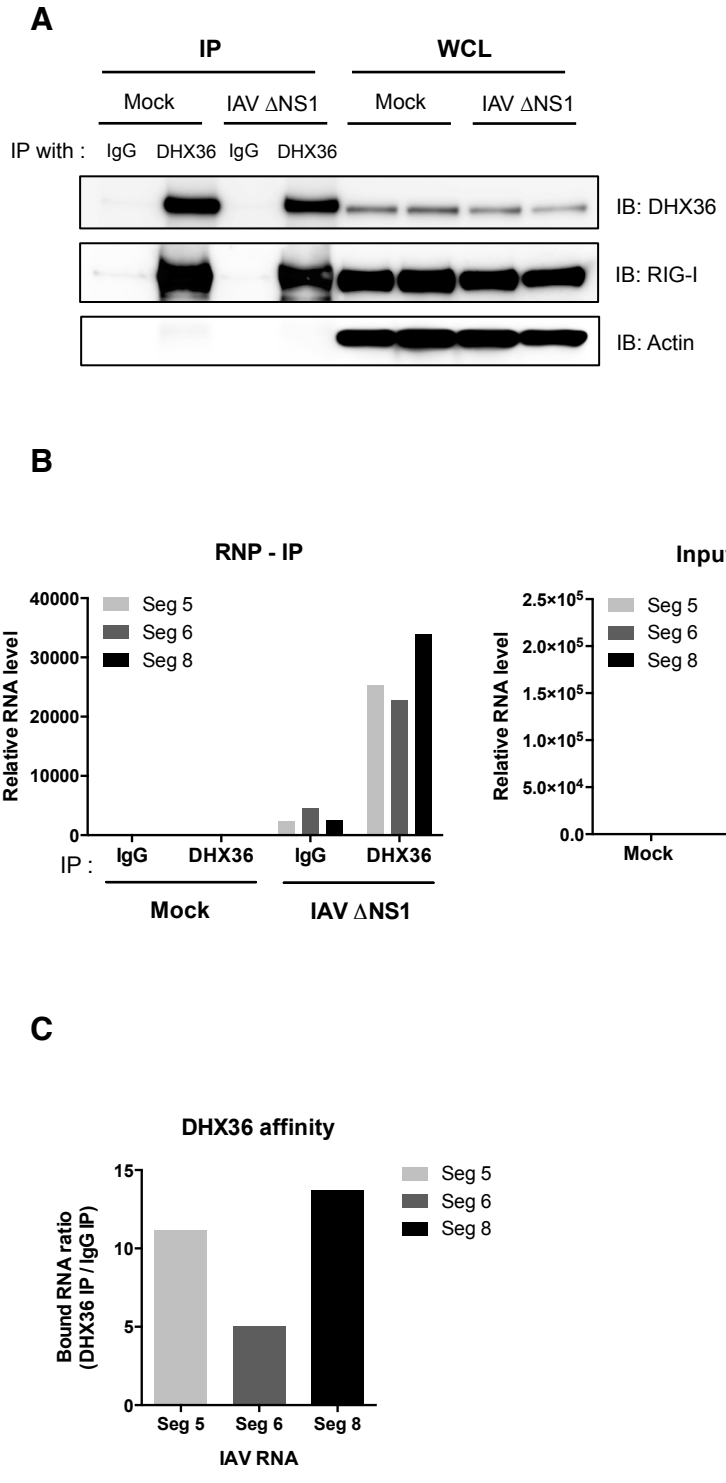

Fig 17. DHX36 recognizes IAV RNA

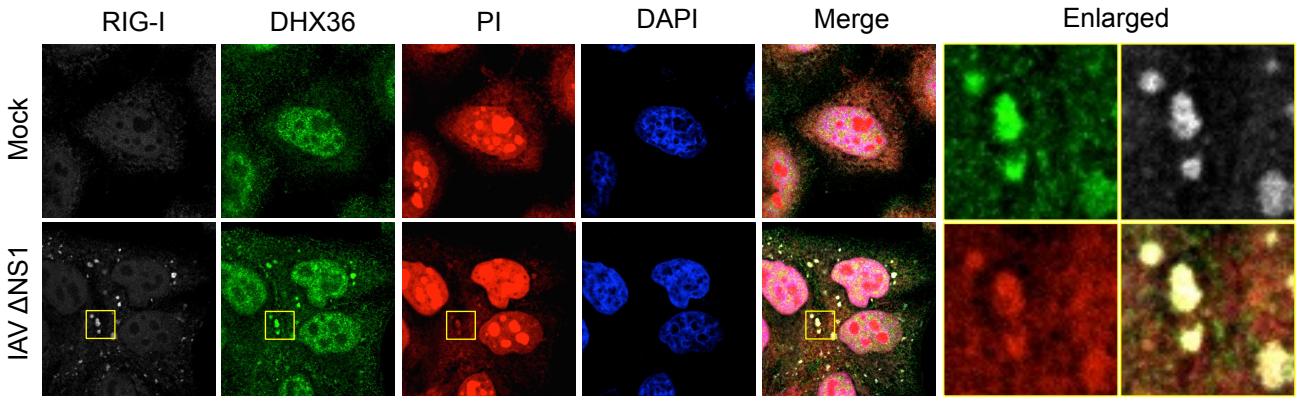

Fig 18. DHX36 and RIG-I co-localize with IAV RNA

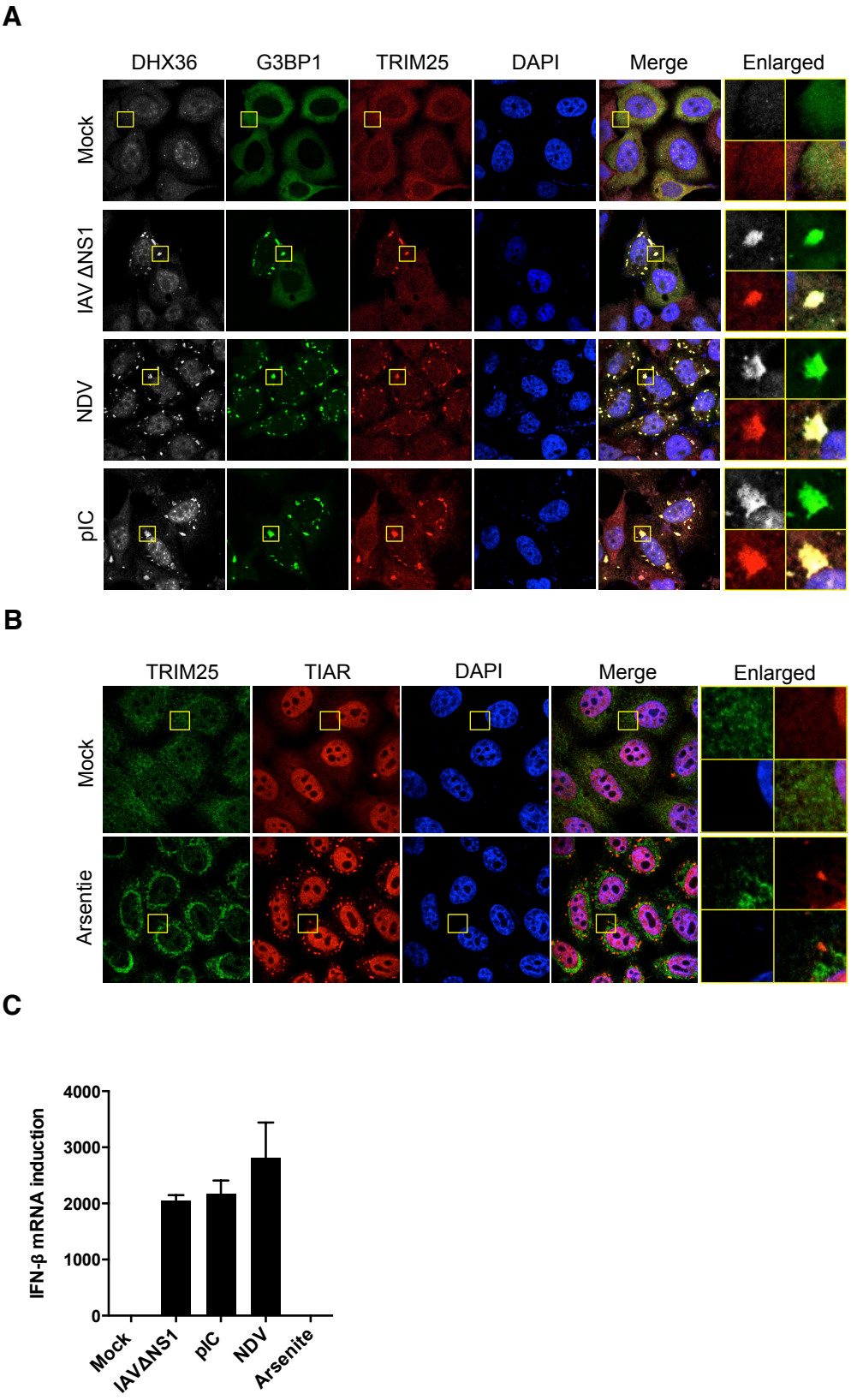

Fig 19. TRIM25 co-localizes with avSG by virus infection or dsRNA transfection

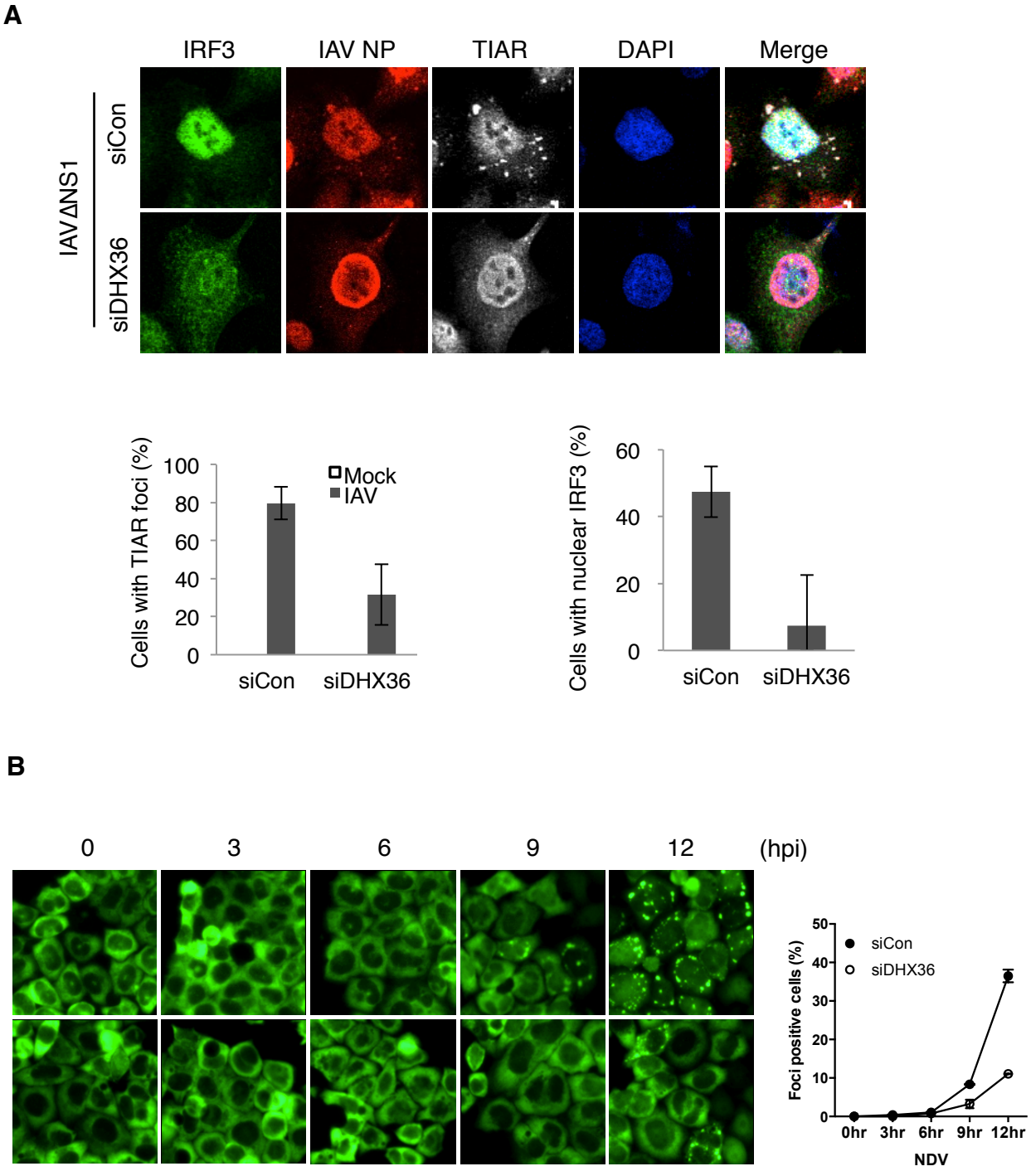

Fig 20. DHX36 mediates avSG formation

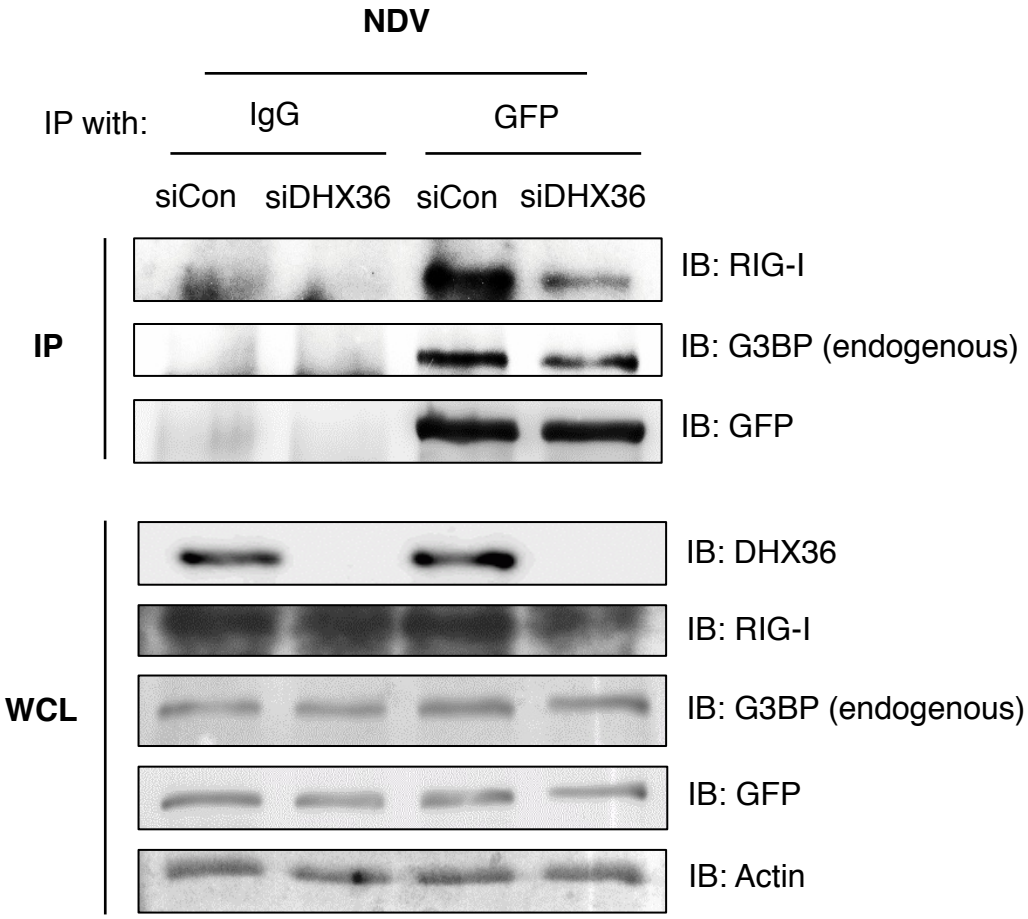

Fig 21. DHX36 affects interaction between RIG-I and G3BP1

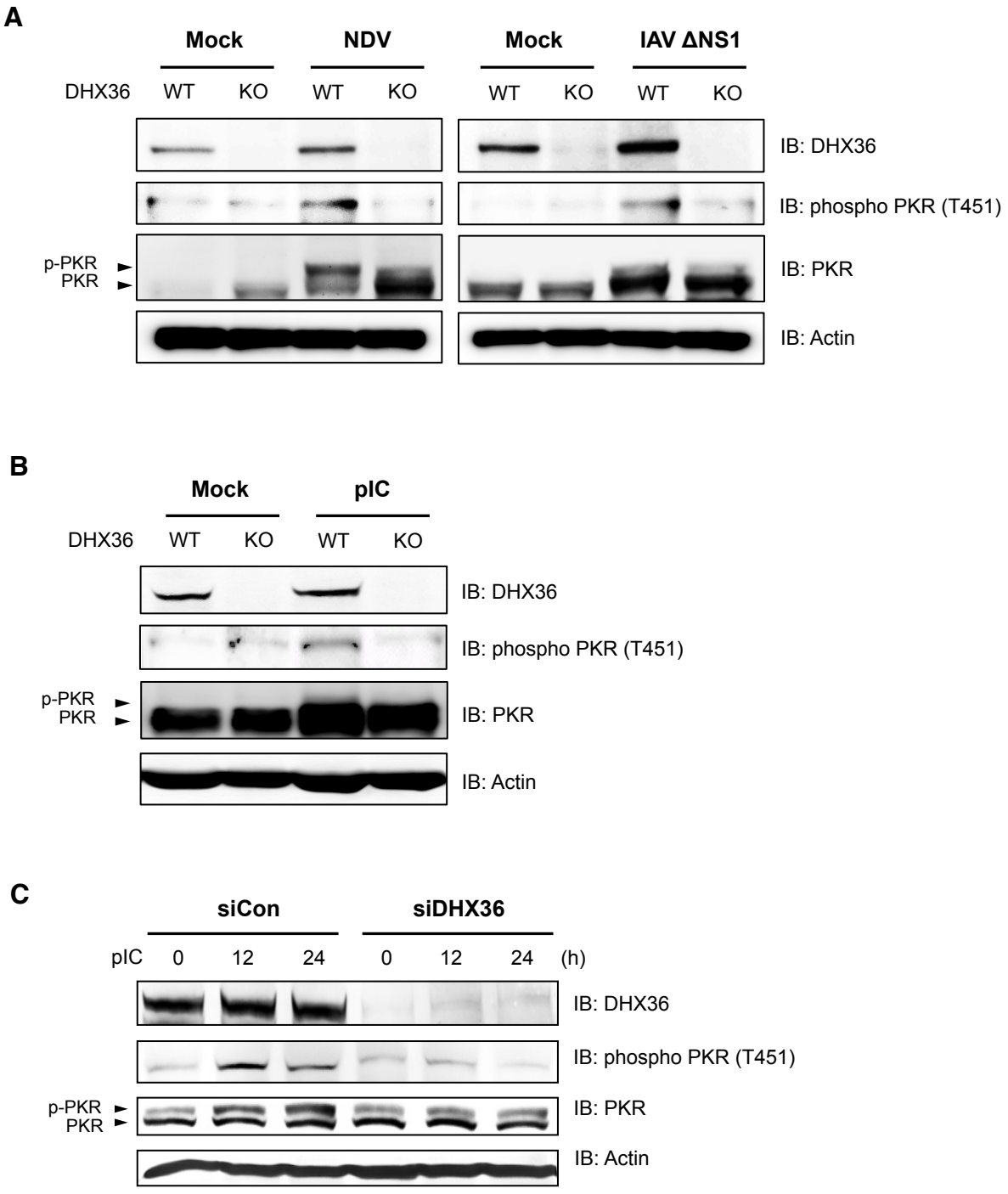

Fig 22. DHX36 facilitates PKR phosphorylation by virus infection or dsRNA transfection

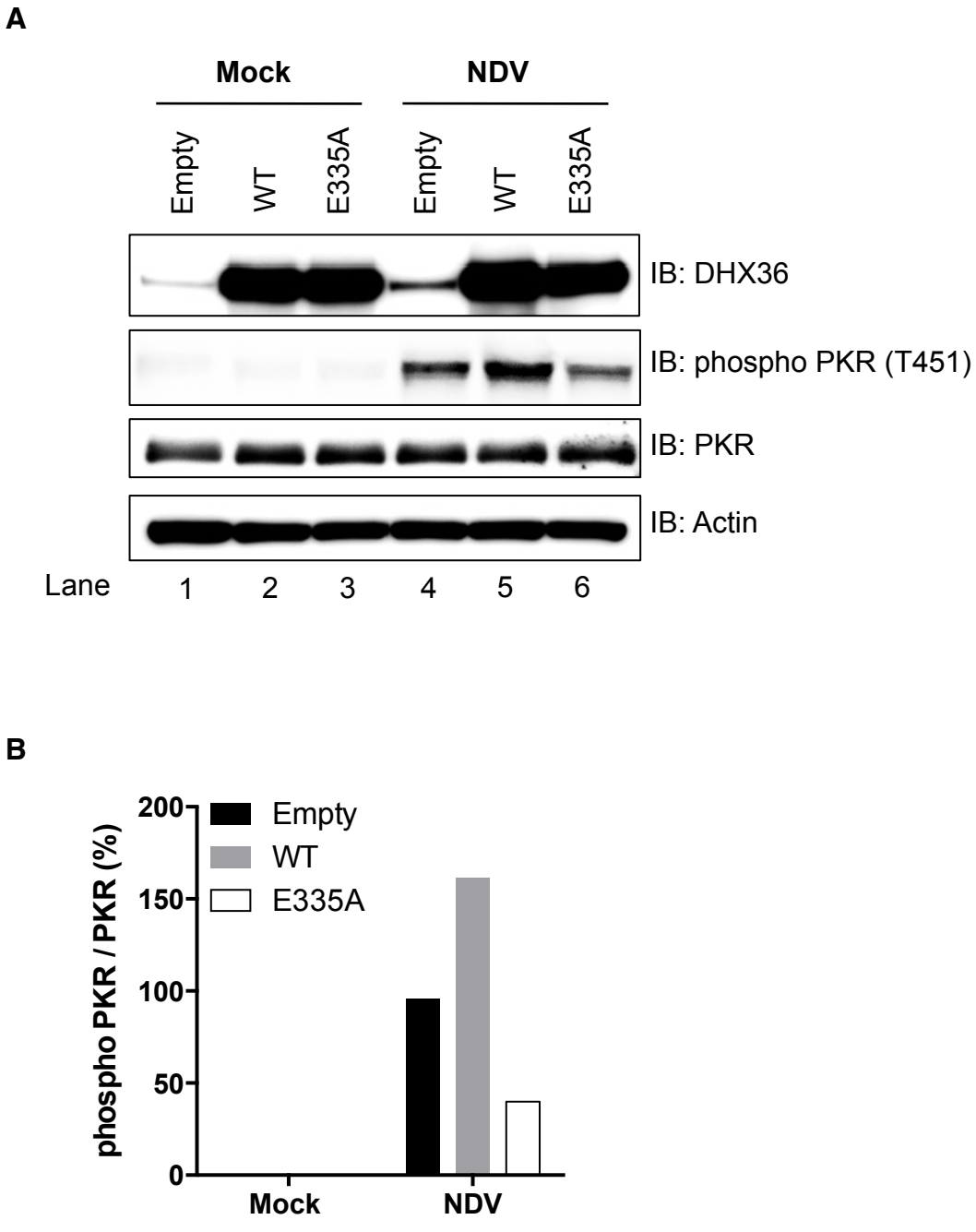

Fig 23. ATPase activity of DHX36 is involved in the regulation of PKR activation

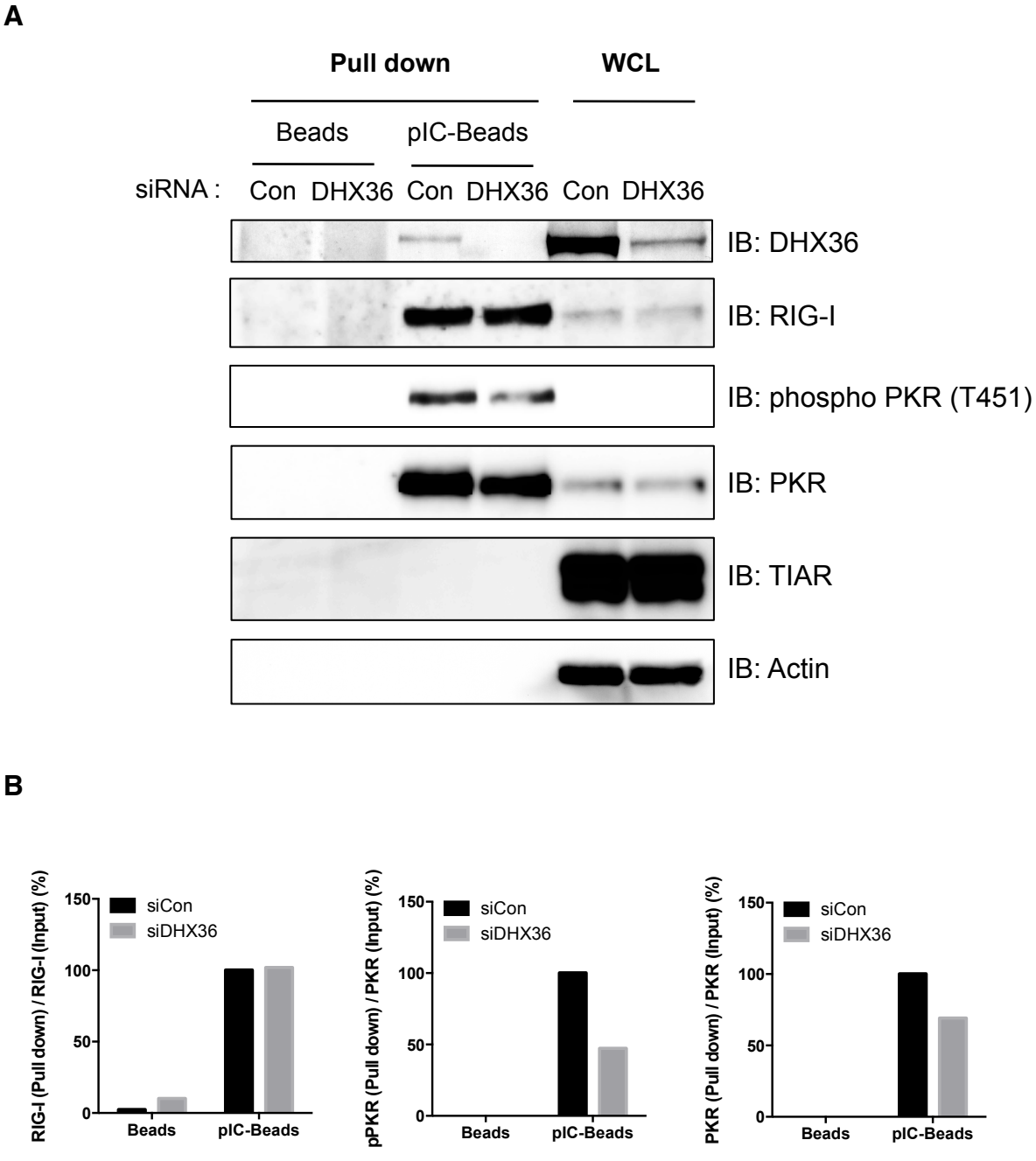

Fig 24. DHX36 affects the binding affinity of PKR to dsRNA

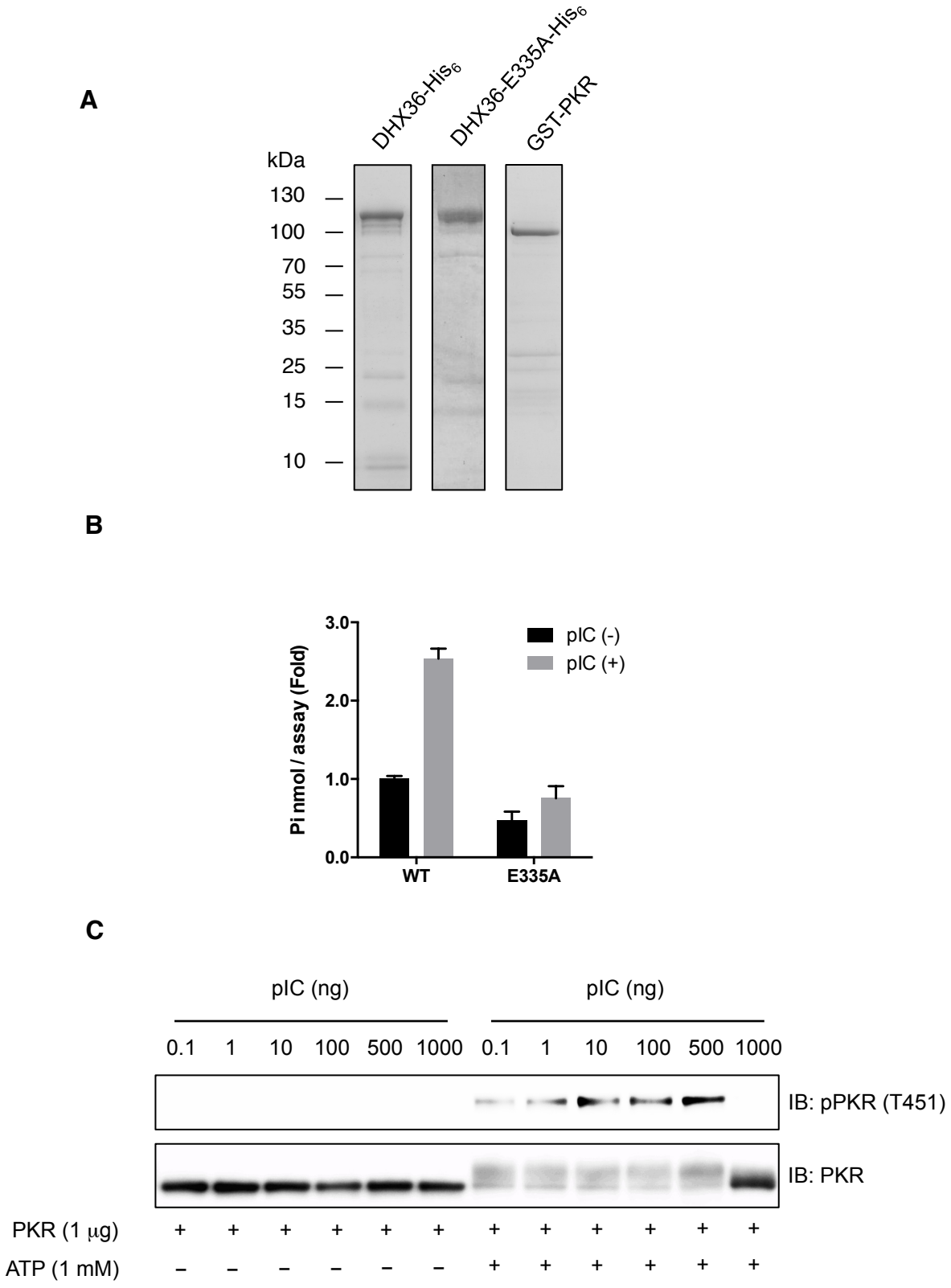

Fig 25. Expression and functional analysis of recombinant DHX36 and PKR

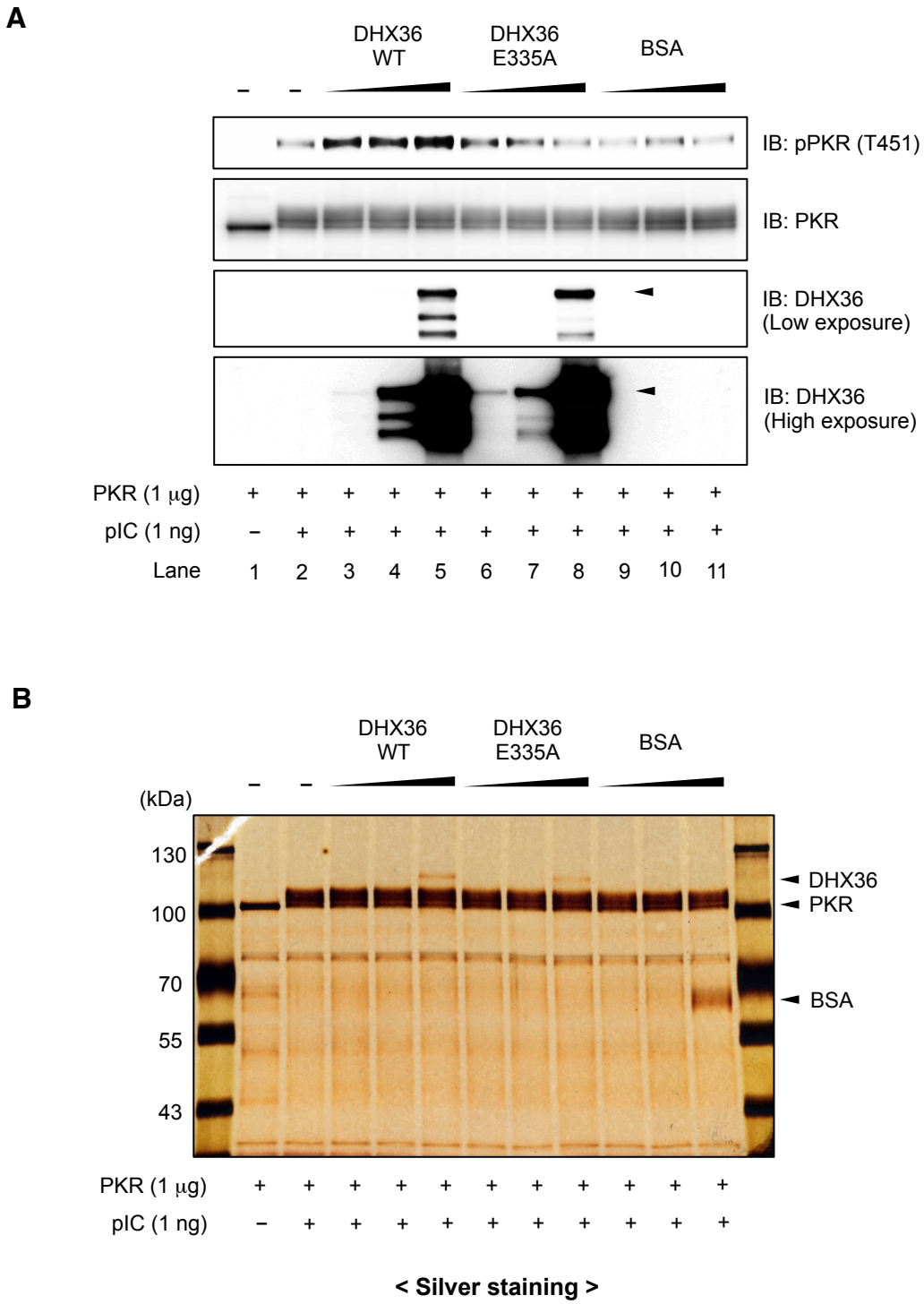

Fig 26. DHX36 facilitates PKR phosphorylation

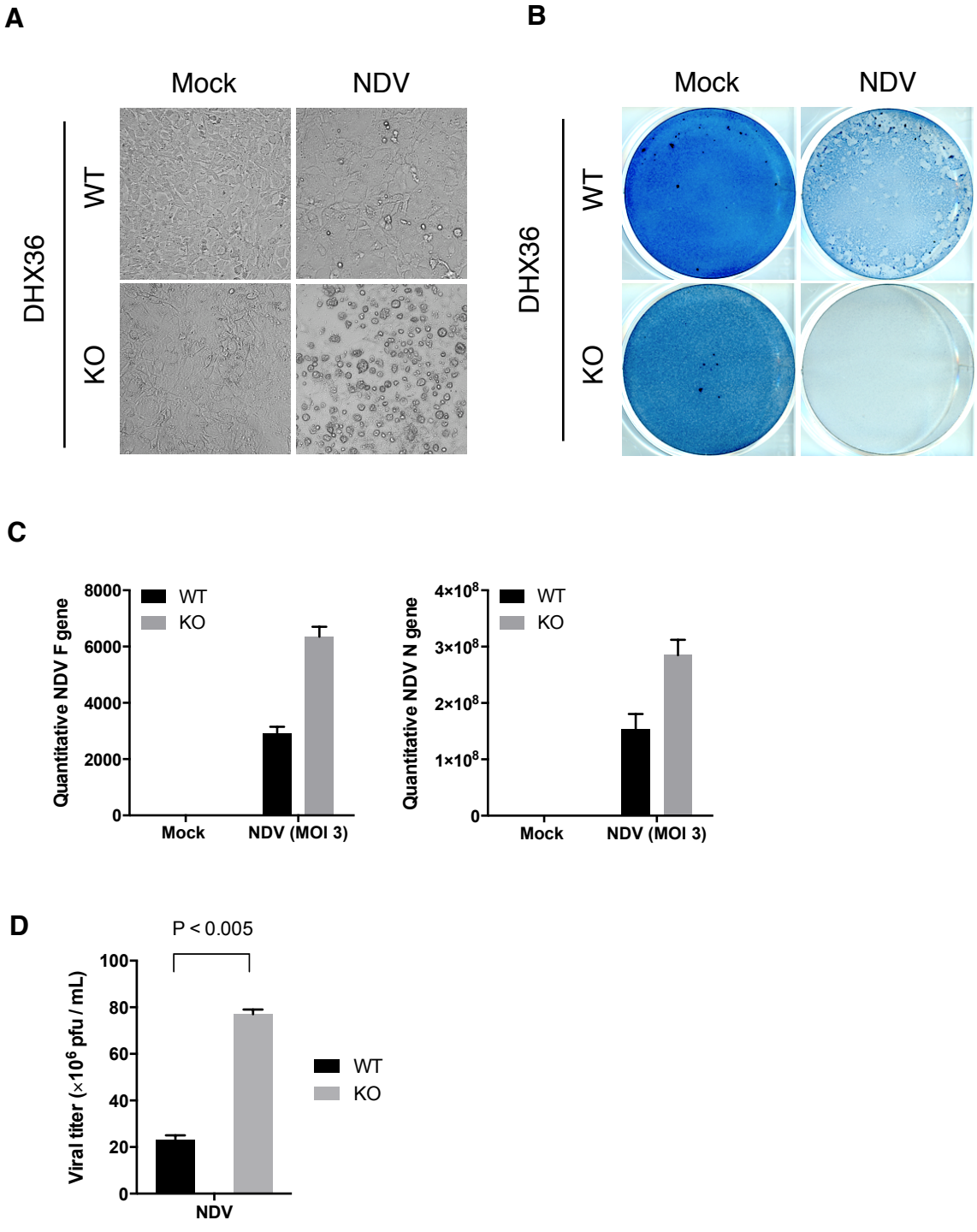

Fig 27. DHX36 exerts its antiviral activity

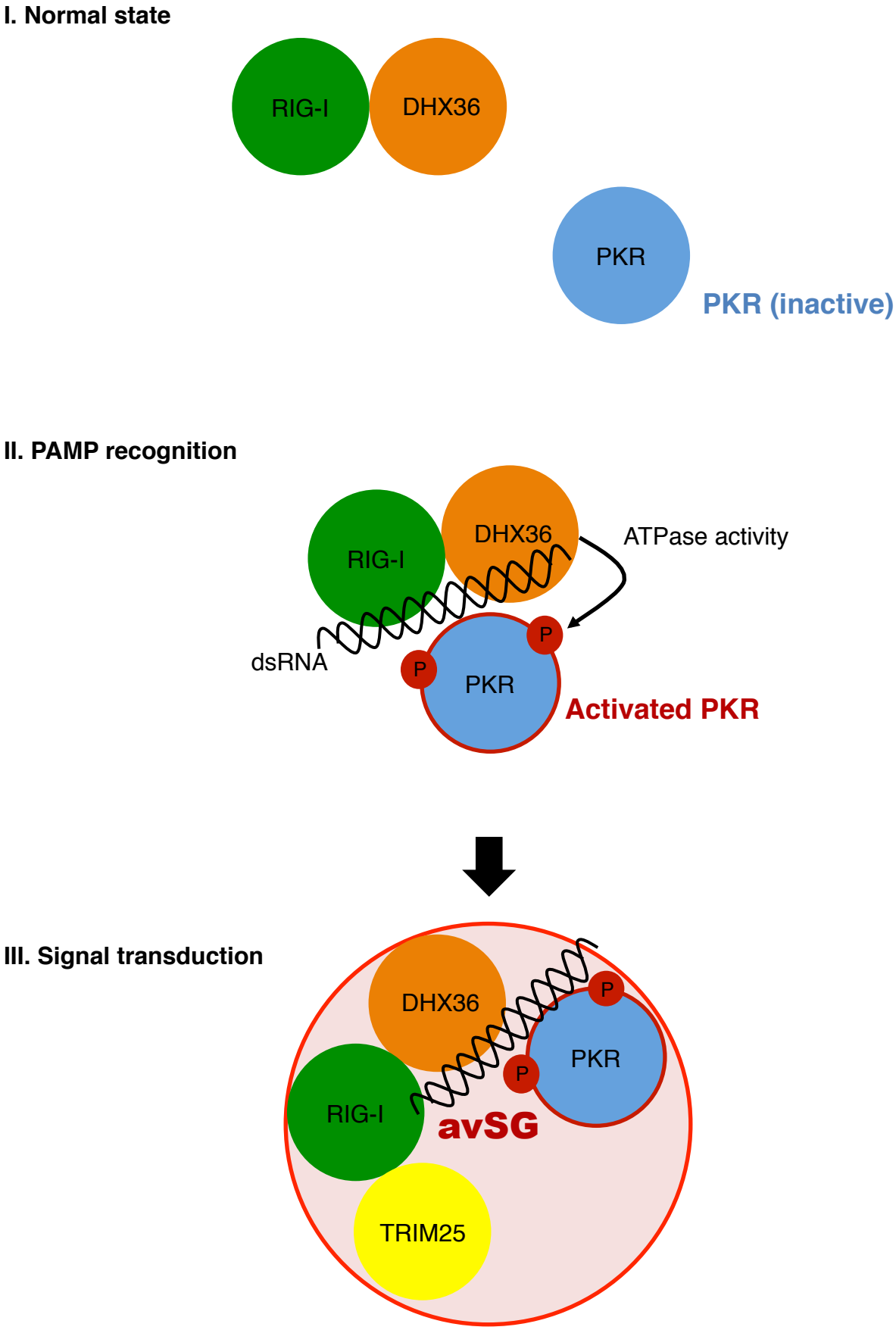

Fig 28. Hypothetical model

Remarks

This thesis is based on material contained in the following scholarly paper.

Ji-Seung Yoo, Kiyohiro Takahasi, Chen Seng Ng, Ryota Ouda, Koji Onomoto, Mitsutoshi Yoneyama, Janice Ching Lai, Simon Lattmann, Yoshikuni Nagamine, Tadashi Matsui, Kuniyoshi Iwabuchi, Hiroki Kato, and Takashi Fujita

DHX36 Enhances RIG-I Signaling by Facilitating PKR-mediated Antiviral Stress Granule Formation

PLoS Pathogens
(March 20, 2014, DOI: 10.1371/journal.ppat.1004012)